eLife

Reviewed Preprint
v2 • September 4, 2024
Revised by authors

Reviewed Preprint
v1 • August 7, 2024

Cell Biology

A *Ctnnb1* enhancer transcriptionally regulates Wnt signaling dosage to balance homeostasis and tumorigenesis of intestinal epithelia

Xiaojiao Hua, Chen Zhao, Jianbo Tian, Junbao Wang, Xiaoping Miao, Gen Zheng, Min Wu, Mei Ye, Ying Liu ✉, Yan Zhou ✉

Department of Neurosurgery, Medical Research Institute, Zhongnan Hospital of Wuhan University, Wuhan University, Wuhan, China • Frontier Science Center of Immunology and Metabolism, Wuhan University, Wuhan, China • Department of Epidemiology and Biostatistics, School of Public Health, Wuhan University, Wuhan, China • TaiKang Center for Life and Medical Sciences, Wuhan University, Wuhan, China • Department of Gastroenterology, Union Hospital, Tongji Medical College, Huazhong University of Science and Technology, Wuhan, China • College of Life Sciences, Wuhan University, Wuhan, China • Department of Gastroenterology, Zhongnan Hospital of Wuhan University, Wuhan, China

Abstract

The β-catenin-dependent canonical Wnt signaling is pivotal in organ development, tissue homeostasis, and cancer. Here we identified an upstream enhancer of *Ctnnb1* – the coding gene for β-catenin, named ieCtnnb1 (intestinal enhancer of *Ctnnb1*), which is crucial for intestinal homeostasis. ieCtnnb1 is predominantly active in the base of small intestinal crypts and throughout the epithelia of large intestine. Knockout of ieCtnnb1 led to a reduction in *Ctnnb1* transcription, compromising the canonical Wnt signaling in intestinal crypts. Single-cell sequencing revealed that ieCtnnb1 knockout altered epithelial compositions and potentially compromised functions of small intestinal crypts. While deletion of ieCtnnb1 hampered epithelial turnovers in physiologic conditions, it prevented occurrence and progression of Wnt/β-catenin-driven colorectal cancers. Human ieCTNNB1 drove reporter gene expression in a pattern highly similar to mouse ieCtnnb1. ieCTNNB1 contains a single-nucleotide polymorphism associated with *CTNNB1* expression levels in human gastrointestinal epithelia. The enhancer activity of ieCTNNB1 in colorectal cancer tissues was stronger than that in adjacent normal tissues. HNF4*α* and phosphorylated CREB1 were identified as key trans-factors binding to ieCTNNB1 and regulating *CTNNB1* transcription. Together, these findings unveil an enhancer-dependent mechanism controlling the dosage of Wnt signaling and homeostasis in intestinal epithelia.

eLife assessment

Ctnnb1 encodes β-catenin, an essential component of the canonical Wnt signaling pathway. In this **important** study, the authors identify an upstream enhancer of Ctnnb1 responsible for the specific expression level of β-catenin in the gastrointestinal track. Deletion of this enhancer in mice and analyses of its association with human colorectal tumors provide **compelling** support that it controls the dosage of Wnt signaling critical to the homeostasis in intestinal epithelia and colorectal cancers.

https://doi.org/10.7554/eLife.98238.2.sa4

Introduction

The gastrointestinal (GI) epithelium, a high turnover organ, contains multiple cell types to fulfill complex functions including food digestion, nutrient absorption, pathogen insulation and clearance, as well as endocrine roles (Noah et al., 2011; Chin et al., 2017; Kurokawa et al., 2020). Enterocytes (ECs) constitute ~90% of all differentiated cells and function as highly efficient cells for absorbing nutrients and water (Snoeck et al., 2005). Goblet cells (GCs) produce mucus to lubricate the mucosal surface (Gustafsson & Johansson, 2022). Enteroendocrine cells (EECs) sense luminal nutrients and secrete peptide hormones to regulate appetite, intestinal motility, and insulin release (Gribble & Reimann, 2019). Tuft cells (TCs) are chemosensory cells that respond to various stimuli including infections and hypoxia (Schneider et al., 2019). The crypts of GI epithelium harbor various types of stem cells that continually replenish lost epithelial cells (van der Flier & Clevers, 2009; Ramadan et al., 2022). While the prevailing belief is that *Lgr5*-expressing crypt base columnar (CBC) cells are actively dividing stem cells and *Bmi*-expressing " +4 " cells (positioned four cells above the base of the crypt) are slowly cycling stem cells, it's important to note that crypt cells have the capacity for fate reprogramming and de-differentiation to sustain regenerative capability (Barker et al., 2007; Tian et al., 2011; Yan et al., 2012; Metcalfe et al., 2014; Beumer & Clevers, 2016). Intestinal stem cells generate transit-amplifying cells (TACs), which undergo multiple cell divisions and differentiate into all intestinal lineages while migrating towards the crypt orifice (Krausova & Korinek, 2014). In addition to stem and progenitor cells, the base of small intestinal crypts contains Paneth cells (PCs) that secret antimicrobial peptides, called defensins, thereby contributing to host defense against microbes (Lueschow & McElroy, 2020; Barreto et al., 2022). PCs also contribute to the stem cell niche function, *e.g.* secreting Wnt ligands, to maintain epithelial homeostasis of the small intestine (Sato et al., 2011).

The behavior of crypt cells is precisely regulated by multiple signals, which can act sequentially, additively, synergistically, or antagonistically (Nakamura et al., 2007). Among them, the Wnt/β-catenin signal pathway represents the principal force governing intestinal epithelium homeostasis, particularly in the preservation of stem cell proliferation and multipotency (Pinto et al., 2003; Clevers et al., 2014; Mah et al., 2016). Upon Wnt ligand binding, the β-catenin degradation complex is inactivated, leading to accumulation of β-catenin and its translocation into the nucleus, where it works with the co-activator TCF7L2 to turn on the transcription of a plethora of target genes, including *MYC*, *CCND1*, *AXIN2*, and *CD44* (Clevers, 2006; Clevers & Nusse, 2012; Nusse & Clevers, 2017). Inhibition of Wnt ligand secretion reduced number of functional stem cells and led to a faster crypt fixation rate (Huels et al., 2018). In the process of aging, reduced Wnt signaling in stem cells and the niche of intestinal crypts causes inhibition of proliferation and reduced numbers of intestinal stem cells (Nalapareddy et al., 2017;

Pentinmikko et al., 2019). The Wnt signal is also essential for commitment, maturation, and location of PCs and other secretory cells (van Es et al., 2005; Andreu et al., 2008). On the other hand, Wnt, EGF and Delta-like 1/4 ligands presented by PCs sustained CBCs' proliferative states and the production (Sato et al., 2011). Although the Wnt signal dosage, largely *via* post-translational regulations, controls early lineage specification, hematopoiesis, and tumorigenesis (Luis et al., 2011; Bakker et al., 2013), it remains elusive how Wnt signaling dosage, particularly through the transcriptional control of *Ctnnb1* – the coding gene for β-catenin, regulates composition and function of intestinal epithelia.

Aberrant activation of canonical Wnt signaling is associated with GI cancers, most notably colorectal cancer (CRC) (Zhao et al., 2022; Zhu & Li, 2023). Germinal mutations of the *APC* gene, which encodes the negative regulator of β-catenin, underlie the Familial Adenomatous Polyposis (FAP), a hereditary neoplastic syndrome and the pre-cancerous condition for CRC (Cheng et al., 2019; J. Li et al., 2021). Moreover, *APC* is mutated in up to 80% of human sporadic CRCs (J. Li et al., 2021). Inactivation of APC causes enhanced accumulation of β-catenin in nuclei and subsequent activation of proliferative and pro-survival signals in CRC cells (Cheng et al., 2019). However, largely due to lack of specificity, no molecular therapeutic strategy targeting the pathway has been incorporated into CRC treatment. Interestingly, the transcriptional activity of *CTNNB1*, the coding gene for β-catenin, is also enhanced in CRCs (Terrin et al., 2017); however, the underlying mechanism is largely unknown. Dissecting it would facilitate the development of new Wnt/β- catenin targeting means to treat CRC.

Enhancers are essential *cis*-regulatory DNA elements that control spatiotemporal gene expressions during cell fate specification and maintenance (Pachano et al., 2022). Active enhancers are often associated with cell fate specifiers, mostly transcription factors (TFs), and are enriched with specific histone modification such as H3K27ac (acetylated lysine 27 of histone H3) and H3K4me1 (mono-methylated lysine 4) of histone H3 (Jindal & Farley, 2021). Importantly, variations of enhancer sequences often lead to aberrant gene silence and activation, thereby causing developmental anomalies and cancers (Zabidi & Stark, 2016; Sengupta & George, 2017; Kvon et al., 2021). Although numerous putative enhancers have been identified by high-throughput studies, only a fraction of them were functionally annotated (Cosmas D.Arnold, 2013; Y. E. Li et al., 2021; Yao et al., 2022).

The proper expression of essential fate genes in different cell types is often controlled by specific enhancers (Kvon et al., 2021; Pachano et al., 2022). Here we have identified an intestinal enhancer for *Ctnnb1* and name it as ieCtnnb1 (intestinal enhancer of *Ctnnb1*). Reporter mice showed that ieCtnnb1 is predominantly active in the base of small intestinal crypts and across the epithelium of large intestine. Knockout of ieCtnnb1 slows down turnovers of intestinal epithelia at physiology and cancer conditions in a Wnt/β-catenin dependent manner. The human ieCTNNB1 contains a SNP that is associated with *CTNNB1* expression levels in human gastrointestinal epithelia. The enhancer activity of ieCTNNB1 in CRC tissues is higher than that in adjacent normal tissues and positively correlates with *CTNNB1* expression levels. HNF4*α* and phosphorylated CREB1 at serine 133 (p-S133-CREB1) were found to associate with ieCtnnb1 and regulate *Ctnnb1* transcription.

Results

ieCtnnb1 is a gastrointestinal enhancer of *Ctnnb1*

We previously identified an evolutionarily conserved upstream enhancer for *Ctnnb1* – neCtnnb1, which regulates neocortical neurogenesis (Figure 1 - figure supplement 1A). We reasoned that there might be other potential enhancer regions that control *Ctnnb1* expression in a cell-specific manner. Therefore, we scanned upstream regions of *Ctnnb1* for active enhancer properties – open

chromatin with enriched H3K27ac and H3K4me1 – in different tissues using data retrieved from the ENCODE database. Interestingly, we noticed that a region that is 29,068 base pair (bp) upstream of the transcription starting site (TSS) for *Ctnnb1* displayed typical enhancer feature in intestinal tissues and resides in the same topologically associating domain (TAD) with *Ctnnb1* (**Figure 1A**, Figure 1 - figure supplement 2A). The region, named as ieCtnnb1 (intestinal enhancer of *Ctnnb1*), is at open chromatin status (DNase I hypersensitive site) and enriched with H3K27ac and H3K4me1, two histone marks for active enhancers, in 8-week-old mouse small intestine tissue (**Figure 1A**). Importantly, the enrichment of H3K27ac at ieCtnnb1 is also prominent in embryonic intestine and stomach tissue, as well as in adult kidney and liver (Figure 1 - figure supplement 1B and D). In contrast, the enrichment was not detected in non-gastrointestinal tissues such as embryonic and adult brain (Figure 1 - figure supplement 1D). In line with signatures of active enhancers, the enrichment of H3K4me3 and H3K36me3 at ieCtnnb1 is negligible in all examined tissues (**Figure 1A**, Figure 1 - figure supplement 1B and C). Notably, unlike neCtnnb1, the primary sequence of ieCtnnb1 is not conserved among vertebrates (**Figure 1A**, bottom).

We next performed *in vitro* and *in vivo* analyses to validate ieCtnnb1's enhancer activity. First, the 2,153 bp core region (CR), representing the H3K27ac peak region of ieCtnnb1, could drive the expression of luciferase reporter in multiple cell types (Figure 1 - figure supplement 2B). Second, the ieCtnnb1 reporter mice ($H11^{i.enh}$) were constructed by inserting the reporter cassette – 5'-*Shh*'s promoter-ieCtnnb1-CR-*LacZ-iCre*-3' – into the *H11* locus (**Figure. 1B**). Of note, the *Shh* promoter alone at the *H11* locus did not drive the expression of reporter gene in all examined tissue (Kvon et al., 2020). Wholemount β-galactosidase (β-gal) staining of 8-week-old tissues revealed prominent ieCtnnb1-*LacZ* signals along the gastrointestinal (GI) tract. The signal exhibited a proximal-low to distal-high gradient, with the ileum, cecum, and colon showing the strongest signals (**Figure. 1B**, Figure 1 - figure supplement 2C). The stomach and proximal duodenum also displayed reporter activity driven by ieCtnnb1 (**Figure. 1B**, Figure 1 - figure supplement 2C). β-gal staining of intestinal sections revealed that the ieCtnnb1-*LacZ* signal could be visualized at the bottom of small intestinal crypts and in the entire large intestinal epithelia, but is absent in sections of liver, kidney, and spleen (Figure 1 - figure supplement 2D and data not shown). Interestingly, the proximal-low to distal-high gradient of ieCtnnb1-*LacZ* signal along the small intestine corresponds to the expression pattern of β-catenin (Figure 1 - figure supplement 2E).

The transcription activity of ieCtnnb1 is strongest at the bottom of crypts, where *Lgr5*-expressing CBC cells and Paneth cells (PCs) reside. To more precisely elucidate cell types in which ieCtnnb1 is active, we crossed $H11^{i.enh}$ mice with *Lgr5*-EGFP-IRES-CreERT2 (*Lgr5*-EGFP) mice to obtain 8-week-old $H11^{i.enh}$;*Lgr5-EGFP* mice. Small intestinal crypts were respectively harvested from *Lgr5-EGFP* and $H11^{i.enh}$;*Lgr5-EGFP* mice followed by enrichment of both eGFP+ and eGFP-cells (Figure 1 - figure supplement 2F). Quantitative RT-PCR (RT-qPCR) analyses indicated that *LacZ* transcripts could be detected in both eGFP+ and eGFP-crypt cells in $H11^{i.enh}$;*Lgr5-EGFP* mice (Figure 1 - figure supplement 2F). Next, sections of $H11^{i.enh}$ crypts were subjected with β-gal staining followed by immunohistochemistry of OLFM4 (a CBC marker) or lysozyme (a PC marker). Data showed X-gal signals are in close proximity with both OLFM4 and lysozyme (**Figure. 1C**), suggesting that the activity of ieCtnnb1 is present in both CBCs and PCs.

We further examined the ieCtnnb1 activity in GI tracts of postnatal day 7 (P7) pups, when GI epithelia are rapidly expanding. The ieCtnnb1-*LacZ* signals could be visualized in epithelia of P7 small and large intestines, aligning well with the distribution of canonical Wnt signaling illustrated by the BAT-Gal mice (Figure 1 - figure supplement 2G and H). Together, ieCtnnb1 drives transcription in embryonic intestinal epithelia, the base of small intestinal crypts and large intestinal epithelia of adult mice.

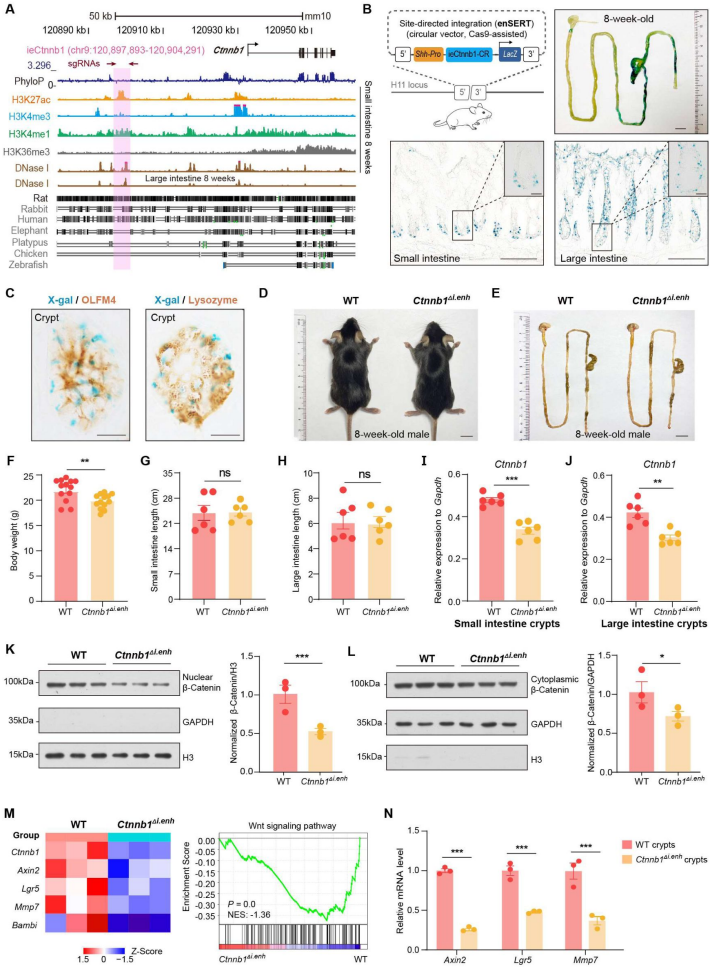

Figure 1.

ieCtnnb1 is an intestinal enhancer of *Ctnnb1*.

(A) Schematic representation of the upstream region of mouse *Ctnnb1* gene and the location of ieCtnnb1 (6,399 bp, pink shading), which is marked by H3K27ac and H3K4me1 peaks, and DNase I hypersensitivity in small intestine and large intestine of 8-week-old mice. The sequence conservation of the indicated species is shown at the bottom as vertical lines. Data were obtained from ENCODE. Locations of single-guide RNAs (sgRNAs) for generating ieCtnnb1 knockout mice were marked. (B) Top left: a schematic illustration showing that the knock-in reporter construct carries the *Shh* promoter, ieCtnnb1 core region sequences (2,153 bp) and the *LacZ* reporter gene. Top right: X-Gal staining (blue) of the gastrointestinal (GI) tract of an 8-week-old $H11^{i.enh}$ mouse. Bottom: X-Gal staining (blue) of the small intestine (left) and colon (right) of an 8-week-old $H11^{i.enh}$ mouse. Boxed areas were enlarged at top-right corners. (C) Representative images of small intestinal crypts co-labelled by X-gal with OLFM4 (left), and X-gal with Lysozyme (right). (D-E) Representative images of whole body (d) and GIs (e) of 8-week-old male wildtype (WT) and $Ctnnb1^{\Delta i.enh}$ mice. (F) Comparison of the body weight of 8-week-old male WT (n = 13) and $Ctnnb1^{\Delta i.enh}$ (n = 13) mice. (G-H) Measurements of small (G) and large (H) intestine length of 8-week-old male WT (n = 6) and $Ctnnb1^{\Delta i.enh}$ (n = 6) mice. (I-J) Relative mRNA levels of *Ctnnb1* in small (I) and large (J) intestinal crypts of WT (n = 6) and $Ctnnb1^{\Delta i.enh}$ (n = 6) mice. (K-L) Left: immunoblotting of nuclear (K) and cytoplasmic (L) β-Catenin, GAPDH and H3 of small intestinal crypts of WT (n = 3) and $Ctnnb1^{\Delta i.enh}$ (n = 3) mice. Right: histograms showing protein levels of β-Catenin normalized to H3 (K) or GAPDH (L) levels. Values of WT were set as '1'. (M) Heat map of indicated Wnt target genes and GSEA analysis of Wnt signaling pathway according to transcriptome profiles of small intestinal crypts of WT (n = 3) and $Ctnnb1^{\Delta i.enh}$ (n = 3) mice. (N) RT-qPCR showing relative mRNA levels of indicated Wnt target genes (*Axin2, Lgr5* and *Mmp7*) in small intestinal crypts of WT (n = 3) and $Ctnnb1^{\Delta i.enh}$ (n = 3) mice. Scale bars, 1 cm (B, top; D and E), 100 μm (B, bottom), 10 μm (B, magnified views; C). Quantification data are shown as means ± SEM, statistical significance was determined using an unpaired two-tailed Student's *t*-test (F-L). Quantification data are shown means ± SD, statistical significance was determined using Multiple *t*-tests - one per row (N). *P < 0.05, **P < 0.01, ***P < 0.001, and ****P < 0.0001. ns, not significant. NES: Normalized Enrichment Score.

ieCtnnb1 knockout decreased the expression of *Ctnnb1* in intestinal epithelia

We next examined whether ieCtnnb1 controls the transcription of *Ctnnb1* in intestinal epithelia. For this purpose, we employed CRISPR/Cas9-mediated gene editing to delete the genomic region containing ieCtnnb1 (Figure 1 - figure supplement 2I). Homozygous ieCtnnb1 knockout ($Ctnnb1^{\Delta i.enh}$) mice were born in Mendelian ratios and thrived through adulthood. Interestingly, the body weight of 8-week-old male $Ctnnb1^{\Delta i.enh}$ mice was slightly but significantly lighter than that of wild-type controls (**Figure. 1D** and **F**), but the length of small and large intestines of $Ctnnb1^{\Delta i.enh}$ mice was comparable to that of control mice (**Figure. 1E, G** and **H**). We then collected crypts from small and large intestine, finding that the expression levels of *Ctnnb1* were decreased by 26.5% and 22.3% respectively in $Ctnnb1^{\Delta i.enh}$ crypts (**Figure. 1I** and **J**). In contrast, the expression level of *Ctnnb1* in the $Ctnnb1^{\Delta i.enh}$ liver remained unaltered (Figure 1 - figure supplement 2J). In addition, the expression of genes located in the same TAD as *Ctnnb1* and ieCtnnb1, including *Ulk4*, *Rpl14* and *Entpd3*, was not changed in $Ctnnb1^{\Delta i.enh}$ small intestinal crypts (Figure 1 - figure supplement 2K). These data suggest that ieCtnnb1 plays a specific role in regulating the transcription of *Ctnnb1* in intestinal epithelia.

In epithelial tissues, most β-Catenin is localized at cell adhesion sites to maintain barrier integrity, while a smaller fraction translocates into the nucleus to activate transcription upon Wnt ligand binding. We therefore carried out nuclear/cytosol fractionation assays, which revealed a substantial decrease in the levels of both nuclear (49.5%) and cytosolic (29.8%) β-Catenin in small intestinal crypts of $Ctnnb1^{\Delta i.enh}$ mice (**Figure. 1K** and **L**). RNA-seq transcriptome and RT-qPCR analyses revealed a significant reduction in the expressions of Wnt target genes in $Ctnnb1^{\Delta i.enh}$ crypts. Additionally, the gene set enrichment analysis (GSEA) showed that the expression levels of many components of the Wnt signaling pathway were also downregulated (**Figure. 1M** and **N**, Figure 1 - figure supplement 3). Together, the loss of ieCtnnb1 compromised the Wnt signaling in intestinal epithelia by reducing *Ctnnb1* transcription.

Loss of ieCtnnb1 altered cellular composition and expression profiles of small intestinal crypts

The canonical Wnt/β-catenin signaling is essential for the construction and homeostasis of intestinal epithelia (Mah et al., 2016). Because ieCtnnb1 maintains the expression level of *Ctnnb1* of intestinal crypts, we investigated how the deletion of ieCtnnb1 affects cellular components and functions of intestinal crypts. We performed single-cell sequencing on EpCAM+ epithelial cells from small intestinal crypts of 10-week-old $Ctnnb1^{\Delta i.enh}$ and control ($H11^{i.enh}$) mice (n = 2 female mice for each genotype) (**Figure. 2A**, Figure 2 - figure supplement 1A) (Ayyaz et al., 2019; Huang et al., 2022). Uniform Manifold Approximation and Projection (UMAP) was employed for dimensionality reduction to cluster cells, then well-established marker genes for intestinal epithelial cells were mapped onto the UMAP representation to designate cell types (Haber et al., 2017; Gu et al., 2022) (**Figure. 2B**, Figure 2 - figure supplement 1B-D). Of note, a small population of crypt cells remains undefined, as we did not exclude non-epithelial cells such as immune cells, erythrocytes, or endothelial cells during the enrichment of EpCAM+ epithelial cells. Additionally, our focus was exclusively on epithelial cell types, and we did not consider other cell types when defining cell populations (Figure 2 - figure supplement 1D). First, in accordance with bulk RNA-seq and RT-qPCR results, the expression levels of *Ctnnb1* were downregulated in almost all $Ctnnb1^{\Delta i.enh}$ crypt cells, and the expression of *Axin2* was decreased in CBCs and TACs (**Figure. 2C** and **D**). Second, the proportion of PCs was decreased by 49.2% in $Ctnnb1^{\Delta i.enh}$ crypts, which was confirmed by the immunohistochemical (IHC) staining of *Defensin 5α*, a PC marker (**Figure. 2E** and **F**). The ieCtnnb1-driving *LacZ* could be detected in the PC cluster (n = 4 10-week-old mice) (Figure 2 - figure supplement 1E). Accordingly, the expression levels of examined PC markers – *Lyz1*, *Pla2g2a*, *Wnt3* and *Math1* – were all significantly compromised in $Ctnnb1^{\Delta i.enh}$

crypts (**Figure. 2G**). The number of goblet cells (GCs) was slightly (not statistically significant) reduced upon loss of ieCtnnb1 (Figure 2 - figure supplement 1F). Third, the proliferative capability of CSCs and TACs were mildly reduced in *Ctnnb1*$^{\Delta i.enh}$ crypts, as the proportion of G2/M cells and the expression of *Mki67* were decreased in the two cell types (**Figure. 2H-J**). Consistently, the numbers of Ki67-positive cells and EdU-labeled cells (4 hours pulse) were decreased by 16.1% and 21.9%, respectively, in *Ctnnb1*$^{\Delta i.enh}$ small intestinal epithelia (**Figure. 2K** and **L**). Fourth, in secretory cells (PCs GCs and EECs), as well as enterocytes/absorptive cells (mature enterocytes (mECs) and immature enterocytes (imECs), and stem cells of *Ctnnb1*$^{\Delta i.enh}$ crypts, the expression of genes related to secretory functions including *Lyz1*, *Ang4*, *Muc2*, and *Mmp7* was decreased. In contrast, the expression of markers for absorptive cells such as *Fabp6*, *Apoa1*, *Fabp2*, and *Reg3b* was elevated (**Figure. 2M** and **N**, Figure 2 - figure supplement 1G). Accordingly, gene ontology (GO) analyses showed in stem cells and secretory cells of *Ctnnb1*$^{\Delta i.enh}$ crypts, upregulated genes were enriched with terms associated with absorptive functions including ribosome biogenesis and oxidative phosphorylation; whereas downregulated genes in stem cells and secretory cells were respectively enriched with terms related to cell division and secretory functions (Figure 2 - figure supplement 1H and I). In contrast, in mECs, downregulated genes were enriched with terms associated with absorptive functions (Figure 2 - figure supplement 1J).

In summary, the loss of ieCtnnb1 results in a reduction in the number of PCs, compromises stem cell proliferation, and disrupts the expression of genes related to secretory and absorptive functions. These effects could be attributed to a combination of reduced Wnt/β-catenin signaling and dysregulated crosstalk among crypt cells.

ieCtnnb1 deletion inhibits tumorigenesis of intestinal cancers by suppressing Wnt/β-catenin signaling

Tumorigenesis of most colorectal cancer (CRC) is associated with aberrant activation of the Wnt/β-catenin signaling (Zhu & Li, 2023). To investigate whether knockout of ieCtnnb1 could suppress the carcinogenesis of Wnt-driven intestinal tumors, we crossbred *Ctnnb1*$^{\Delta i.enh}$ mice with *Apc*$^{Min/+}$ mice. In *Apc*$^{Min/+}$ mice, a nonsense mutation of the *Apc* gene results in the translation of truncated and dysfunctional APC protein, leading to failed degradation and nuclear translocation of β-catenin. *Apc*$^{Min/+}$ mice spontaneously develop intestinal tumors due to enhanced canonical Wnt/β-catenin signaling in the intestinal epithelia, particularly in stem cells (Su et al., 1992). The survival period of *Ctnnb1*$^{\Delta i.enh}$;*Apc*$^{Min/+}$ mice (median survival - 255 days) was significantly longer than the *Apc*$^{Min/+}$ mice (median survival - 165 days), with the former having a heavier body weight (**Figure. 3A** and **C**). Strikingly, the *Ctnnb1*$^{\Delta i.enh}$;*Apc*$^{Min/+}$ mice barely grow colorectal cancers and have much fewer intestinal tumors compared to *Apc*$^{Min/+}$ mice, with significantly smaller tumor area (**Figure. 3B, D-F**, Figure 3 - figure supplement 1A-C). IHC analyses showed that tumors in *Ctnnb1*$^{\Delta i.enh}$;*Apc*$^{Min/+}$ large and small intestines had much fewer Ki67+ proliferating cells, expressed significant less β-catenin, but contained more Muc2-expressing Goblet cells, suggesting *Ctnnb1*$^{\Delta i.enh}$;*Apc*$^{Min/+}$ tumors behave like normal epithelia (**Figure. 3G-L**, Figure 3 - figure supplement 1D-I). Consistently, RNA-seq transcriptome experiments showed that *Ctnnb1*$^{\Delta i.enh}$;*Apc*$^{Min/+}$ colorectal cancers significantly downregulated genes associated with the Wnt signaling pathway, pluripotency of stem cells, and gastric cancer; whereas increased expression of genes related to normal epithelial functions including oxidative phosphorylation, adhesion, protein digestion and absorption, and Mucin biosynthesis (**Figure. 3M-O**). Thus, ablation of ieCtnnb1 deters tumorigenesis of intestinal cancers by suppressing the Wnt signaling.

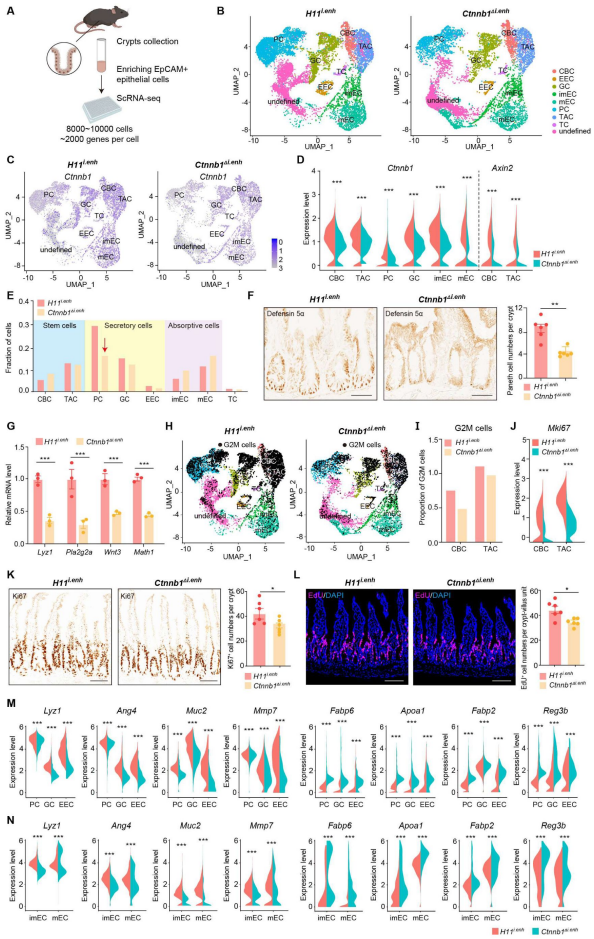

Figure 2.

ieCtnnb1 knockout altered cellular composition and expression profiles of small intestinal crypts.

(A) Schematic illustration of single-cell sequencing. Crypts were extracted from small intestines followed by fluorescence activated cell sorting (FACS) to enrich EpCAM+DAPI-epithelial cells. Cells of two 10-week-old female mice for each genotype were pooled together to perform single cell transcriptome analyses. (B) UMAP were used to visualize the clustering of 11,824 single cells from *H11*$^{i.enh}$ mice and 8,094 single cells from *Ctnnb1*$^{\Delta i.enh}$ mice. Cell types were assigned according to expressions of marker genes. CBC, crypt base columnar cell; TAC, transit amplifying cell; EEC, enteroendocrine cell; imEC, immature enterocytes; mEC, mature enterocytes; GC, goblet cell; PC, Paneth cell; TC, tuft cell. (C) Expression and distribution of *Ctnnb1* in small intestinal crypt cells of *H11*$^{i.enh}$ and *Ctnnb1*$^{\Delta i.enh}$ mice. (D) Violin plots showing the expression of *Ctnnb1* in CBC, TAC, PC, GC, imEC, mEC; and the expression of *Axin2* in CBC and TAC, of *H11*$^{i.enh}$ and *Ctnnb1*$^{\Delta i.enh}$ mice. (E) Comparison of the proportion of indicated small intestinal crypt cell types in *H11*$^{i.enh}$ and *Ctnnb1*$^{\Delta i.enh}$ mice. (F) Immunohistochemistry (left and middle) and quantification (right) of PCs in small intestines of *H11*$^{i.enh}$ (n = 6) and *Ctnnb1*$^{\Delta i.enh}$ (n = 6) mice. (G) RT-qPCR showing relative mRNA levels of PC marker genes (*Lyz1, Pla2g2a, Wnt3, Math1*) in small intestinal crypts of *H11*$^{i.enh}$ (n = 3) and *Ctnnb1*$^{\Delta i.enh}$ (n = 3) mice. (H) Distribution of G2M cells in *H11*$^{i.enh}$ and *Ctnnb1*$^{\Delta i.enh}$ small intestinal crypts, based on the expression of cell cycle marker gene *Mki67*. (I) Comparison of the proportion of G2M cells in CBC and TAC of *H11*$^{i.enh}$ and *Ctnnb1*$^{\Delta i.enh}$ small intestinal crypts. (J) Violin plots showing the expression of *Mki67* in CBC and TAC of *H11*$^{i.enh}$ and *Ctnnb1*$^{\Delta i.enh}$ small intestinal crypts. (K) Immunohistochemistry (left and middle) and quantification (right) of Ki67+ cells in small intestines of *H11*$^{i.enh}$ (n = 6) and *Ctnnb1*$^{\Delta i.enh}$ (n = 6) mice. (L) Immunofluorescence (left and middle) and quantification (right) of EdU+ cells (red) in small intestines of *H11*$^{i.enh}$ (n = 6) and *Ctnnb1*$^{\Delta i.enh}$ (n = 6) mice after 4 hours EdU injection. Nuclei were labeled with DAPI (blue). (M-N) Violin plots showing expressions of marker genes for secretory cells (*Lyz1, Ang4, Muc2, Mmp7*) and absorptive cells (*Fabp6, Apoa1, Fabp2, Reg3b*) in secretory(M) and absorptive lineages (N) of *H11*$^{i.enh}$ and *Ctnnb1*$^{\Delta i.enh}$ small intestinal crypts. Scale bars, 50 μm (F, K, and L). Quantification data are shown as means ± SEM, statistical significance was determined using an unpaired two-tailed Student's *t*-test (D, F, J, K, L, M and N). Quantification data are shown means ± SD, statistical significance was determined using Multiple *t*-tests - one per row (G). *P < 0.05, **P < 0.01, ***P < 0.001, and ****P < 0.0001. ns, not significant.

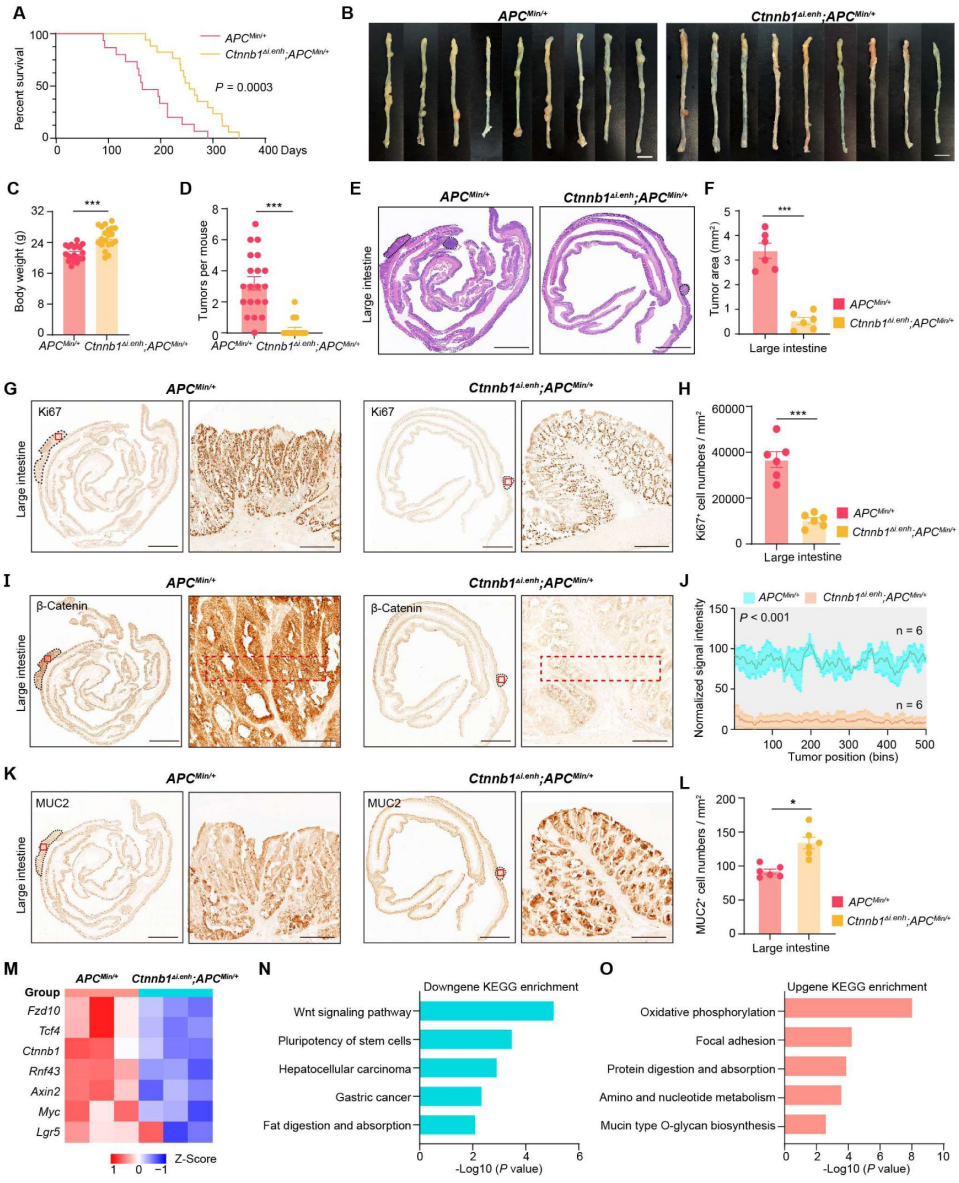

Figure 3.

Knocking out ieCtnnb1 inhibits tumorigenesis of colorectal cancer.

(A) Survival of *Apc*$^{Min/+}$ (n = 15) and *Ctnnb1*$^{\Delta i.enh}$;*Apc*$^{Min/+}$ (n = 17) mice. (B) Colon images of 5-month-old *Apc*$^{Min/+}$ (n = 9) and *Ctnnb1*$^{\Delta i.enh}$;*Apc*$^{Min/+}$ (n = 9) mice. (C) Weight statistics of 5-month-old *Apc*$^{Min/+}$ (n = 20) and *Ctnnb1*$^{\Delta i.enh}$;*Apc*$^{Min/+}$ (n = 20) mice. (D) The statistical analysis of tumor counts in colons of 5-month-old *Apc*$^{Min/+}$ (n = 9) and *Ctnnb1*$^{\Delta i.enh}$;*Apc*$^{Min/+}$ (n = 9) mice. (E) Representative H&E staining images of colon sections of 5-month-old *Apc*$^{Min/+}$ and *Ctnnb1*$^{\Delta i.enh}$;*Apc*$^{Min/+}$ mice. (F) The statistical analysis of colon tumor area in 5-month-old *Apc*$^{Min/+}$ (n = 6) and *Ctnnb1*$^{\Delta i.enh}$;*Apc*$^{Min/+}$ (n = 6) mice. (G-H) Immunohistochemistry (G) and quantification (H) of Ki67+ cells in colon tumors of 5-month-old *Apc*$^{Min/+}$ (n = 6) and *Ctnnb1*$^{\Delta i.enh}$;*Apc*$^{Min/+}$ (n = 6) mice. (I-J) Immunohistochemistry (I) and signal intensity statistics (J, red dashed boxes of I) of β-Catenin in colon tumors of 5-month-old *Apc*$^{Min/+}$ (n = 6) and *Ctnnb1*$^{\Delta i.enh}$;*Apc*$^{Min/+}$ (n = 6) mice. (K-L) Immunohistochemistry (K) and quantification (L) of MUC2+ cells in colon tumors of 5-month-old *Apc*$^{Min/+}$ (n = 6) and *Ctnnb1*$^{\Delta i.enh}$;*Apc*$^{Min/+}$ (n = 6) mice. (M) The heat map showing relative expressions of Wnt signaling pathway genes of colon tumors from 5-month-old *Apc*$^{Min/+}$ (n = 3) and *Ctnnb1*$^{\Delta i.enh}$;*Apc*$^{Min/+}$ (n = 3) mice. (N-O) KEGG analyses of downregulated (N) and upregulated (O) genes in colon tumors of 5-month-old *Apc*$^{Min/+}$ (n = 3) and *Ctnnb1*$^{\Delta i.enh}$;*Apc*$^{Min/+}$ (n = 3) mice. Scale bars, 1 cm (B), 4 mm (E, G, I and K), 200 μm (magnified views in G and K), 100 μm (magnified views in I). Quantification data are shown as means ± SEM, statistical significance was determined using an unpaired two-tailed Student's *t*-test (C, D, F, H, J and L) or log-rank analysis (A). *P < 0.05, **P < 0.01, ***P < 0.001, and ****P < 0.0001. ns, not significant.

Human ieCTNNB1 drives the expression of reporter gene in the gastrointestinal tract

We next investigated whether the human genome also harbors an intestinal enhancer for *CTNNB1*. A region with open chromatin (DNase I hypersensitivity) and enrichment of H3K27ac/H3K4me1 was identified at 38,489 bp upstream of human *CTNNB1* in adult small intestine and colon tissues (**Figure. 4A**). Moreover, the H3K27ac enrichment is also present in esophagus but not in non-GI tissues (Figure 4 - figure supplement 1A). Similar to ieCtnnb1, the 3 kb-long human genomic region, named as ieCTNNB1, resides in the same TAD as the promoter of *CTNNB1* (Figure 4 - figure supplement 1B). We generated ieCTNNB1 reporter mice ($H11^{hi.enh}$) and observed that ieCTNNB1 could drive *LacZ* expression in the bottom of small intestinal crypts and the entire epithelia of large intestine, also exhibiting a proximal-low to distal-high pattern (**Figure. 4B**). Notably, the LacZ signal driven by human ieCTNNB1 was less intense than that driven by mouse ieCtnnb1, potentially attributed to species-specific TF-enhancer interactions.

The H3K27ac-enriched region of ieCTNNB1 was divided into five equal parts for the luciferase reporter assay. Experiments demonstrated that each of the five ieCTNNB1 subregions individually increased luciferase activity in both HCT116 and HeLa cells (**Figure. 4C**, Figure 4 - figure supplement 1C). We then conducted CRISPR mediated activation and interference in HCT-15 colorectal cancer cells using three guide RNAs (gRNAs) targeting ieCTNNB1, which respectively enhanced and inhibited transcription of *CTNNB1* (**Figure. 4D**). Together, ieCTNNB1 is the intestinal enhancer of *CTNNB1* for human GI epithelia.

ieCTNNB1 is activated in colorectal cancer and its activity positively correlates with the expression of *CTNNB1*

CRC, one of the most prevalent cancers in human, is often associated with aberrant activation of the Wnt signaling (J. Li et al., 2021). We then studied whether the occurrence of CRC is associated with enhancer activation of ieCTNNB1. We previously conducted paired analyses of chromatin immunoprecipitation sequencing (ChIP-seq) for H3K27ac and H3K4me3, alongside RNA-seq on 68 CRC samples and their adjacent normal (native) tissue (Q. L. Li et al., 2021). In the current study, we performed analyses for the enrichment of H3K27ac and H3K4me3 at ieCTNNB1 and *CTNNB1* promoter regions, as well as the expression levels of *CTNNB1*, followed by combined analyses (**Figure. 5A**, Figure 5 - figure supplement 1). As anticipated, the expression levels of *CTNNB1* in CRC samples were significantly higher than those in neighboring native tissues (**Figure. 5B**). Essentially, the enrichment of H3K27ac at ieCTNNB1 in CRC tissues were significantly higher than that in native tissues (**Figure. 5C**, Figure 5 – figure supplement 1A). In contrast, the enrichment of H3K4me3 at *CTNNB1*'s promoter was comparable between cancer and native tissues (**Figure. 5C**). Moreover, the enrichment of H3K27ac at ieCTNNB1 positively correlated with the expression of *CTNNB1*; but the enrichment of H3K4me3 at *CTNNB1*'s promoter was not associated with *CTNNB1*'s expression (**Figure. 5D**). Therefore, it's the activity of enhancer but not the promoter that reflects the occurrence of CRC and expression levels of *CTNNB1*.

By examining Genotype Tissue Expression (GTEx) eQTL data browser, a single-nucleotide polymorphism (SNP) – rs15981379 (C>T) within ieCTNNB1 was discovered (**Figure. 5A**). Importantly, the C>T variation is inversely correlated with expression levels of *CTNNB1* in the esophagus and transverse colon (**Figure. 5E**). Luciferase reporter assays in HCT116 and HeLa cells revealed that the C>T variation indeed compromised luciferase activity driven by the ieCTNNB1-region 1 (**Figure. 5F**).

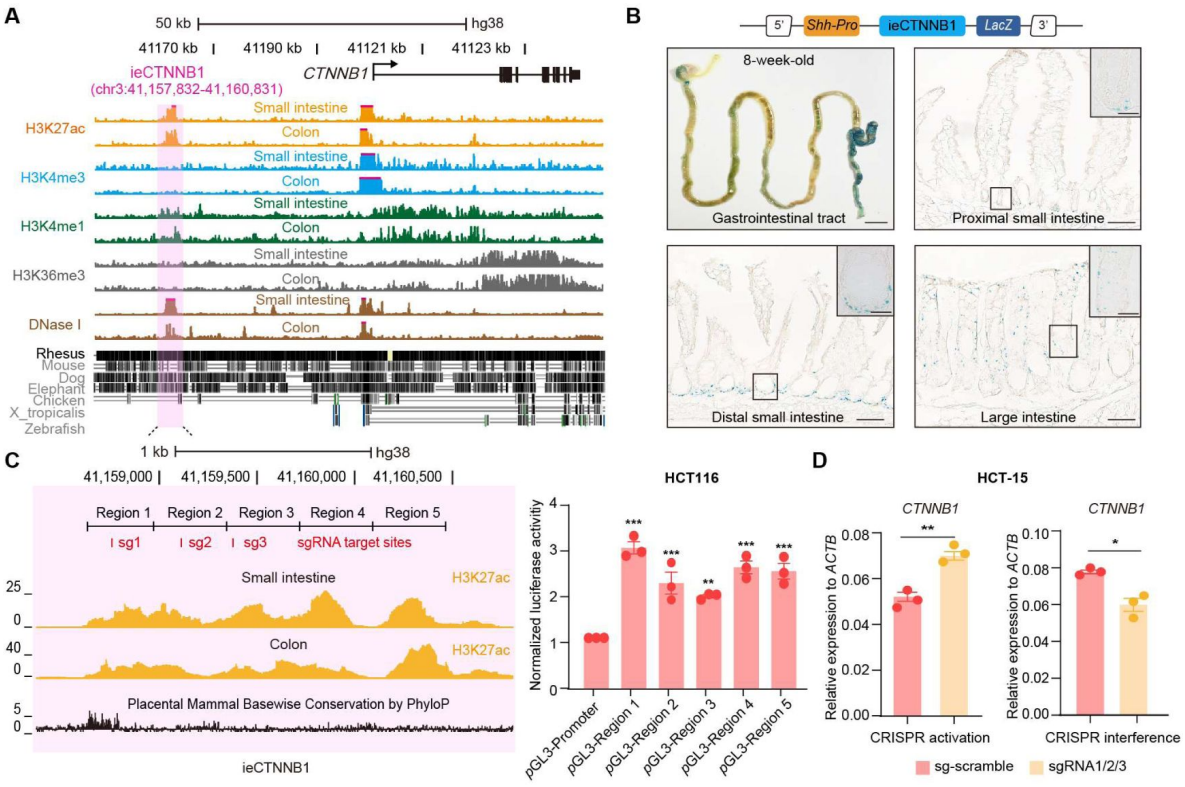

Figure 4.

ieCTNNB1 is the intestinal enhancer of human *CTNNB1*.

(A) Schematic representation of human *CTNNB1* gene and the location of ieCTNNB1 (3,000 bp, pink shading), which is marked by H3K27ac and H3K4me1 peaks, and DNaseI hypersensitivity in human small intestine (30-year-old female) and colon (34-year-old male). Data were obtained from ENCODE. (B) Top: a schematic illustration showing that the knock-in construct containing the *Shh* promoter, ieCTNNB1 sequences (3,000 bp), and the LacZ reporter gene. Bottom: X-Gal staining (blue) of the gastrointestinal tract, and sections of the proximal small intestine, distal small intestine, and large intestine in 8-week-old $H11^{hi.enh}$ mice. (C) Left: ieCTNNB1 is marked by enrichment of H3K27ac in human small intestine (30-year-old female) and colon (34-year-old male). Data were obtained from ENCODE. Locations of sgRNA target sites were indicated. Five subregions of ieCTNNB1 were shown. Right: luciferase reporter assay in HCT116 cells transfected with indicated plasmids for 48 hours. (D) RT-qPCR showing relative mRNA levels of *CTNNB1* in HCT-15 cells transfected with indicated CRISPR activation or CRISPR interference vectors for 48 hours. Scale bars, 1 cm (whole mount in B), 100 μm (sections in B), 10 μm (magnified views in B). Quantification data are shown as means ± SEM, statistical significance was determined using one-way ANOVA analysis (C) and an unpaired two-tailed Student's *t*-test (D). **P* < 0.05, ***P* < 0.01, ****P* < 0.001, and *****P* < 0.0001. ns, not significant.

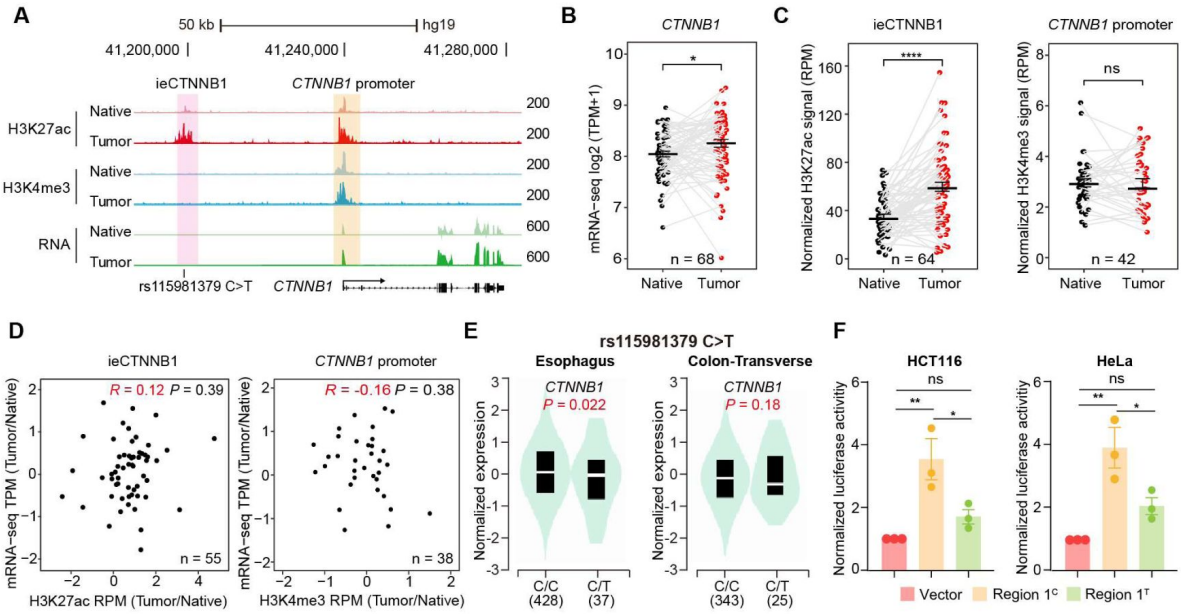

Figure 5.

ieCTNNB1 is activated in colorectal cancer and its activity positively correlates with the expression of *CTNNB1*.

(A) Schematic representation of ieCTNNB1 (pink shading) and *CTNNB1* promoter (yellow shading), which is respectively marked by H3K27ac and H3K4me3 peaks, and mRNA signals in native and tumor tissues of a patient with colorectal cancer. The location of risk mutation site was indicated. (B) Comparison of *CTNNB1* expression levels in native and tumor tissues of colorectal cancer patients (n = 68). (C) Left: comparison of H3K27ac signals at ieCTNNB1 in native and tumor tissues of colorectal cancer patients (n = 64). Right: comparison of H3K4me3 signals at *CTNNB1* promoter in native and tumor tissues of colorectal cancer patients (n = 42). (D) Left: correlation between H3K27ac signals at ieCTNNB1 and *CTNNB1* expression in native and tumor tissues of colorectal cancer patients (n = 55). Right: correlation between H3K4me3 signals at *CTNNB1* promoter and *CTNNB1* expression in native and tumor tissues of colorectal cancer patients (n = 38). (E) Left: comparison of *CTNNB1* expression in esophagus between subjects with common sequence (C/C, n = 428) and variant sequence (C/T, n = 37). Right: comparison of *CTNNB1* expression in transverse colon between subjects with common sequence (C/C, n = 343) and variant sequence (C/T, n = 25). (F) Luciferase reporter assay in HCT116 and HeLa cells transfected with indicated plasmids for 48 hours. Quantification data are shown as means ± SEM, statistical significance was determined using a paired (B, C and D) or unpaired (E) two-tailed Student's *t*-test and Two-way ANOVA analysis (F). **P* < 0.05, ***P* < 0.01, ****P* < 0.001, and *****P* < 0.0001. ns, not significant. R: Pearson correlation.

HNF4*α* and p-S133-CREB1 bind to ieCTNNB1 and maintains the expression of *CTNNB1*

Characterizing associated trans-factors of ieCtnnb1 and ieCTNNB1 is essential for revealing related transcriptional mechanisms and holds clinical relevance. By examining Cistrome Data Browser for ChIP-seq data, eight trans-factors were found to associate with ieCTNNB1 in human colorectal cancer cells or ieCtnnb1 in mouse GI tissues (**Figure. 6A**, Figure 6 - figure supplement 1A). Moreover, they are relatively highly expressed and/or have positive correlation with *CTNNB1*'s expression in colon cancer samples. We then transduced shRNAs-expressing plasmids into HCT-15 cells to individually down-regulate their expressions, revealing that decreasing the expression of *CREB1* (cAMP responsive element binding protein 1) or *HNF4A* (hepatocyte nuclear factor 4 alpha) could compromise *CTNNB1*'s transcription (**Figure. 6B**, Figure 6 - figure supplement 1B). Of note, HNF4*α* plays crucial roles in the normal development of the colon and the maintenance of epithelial barrier (Garrison et al., 2006; Cattin et al., 2009). The phosphorylation of CREB1 at serine 133 (p-S133-CREB1) is essential for its role in activation of gene transcription (Carlezon et al., 2005). ChIP-qPCR experiments showed that enrichment of p-S133-CREB1 was more prominent than CREB1 at ieCtnnb1 in small intestinal crypts and at ieCTNNB1 in HCT-15 cells (**Figure. 6C** and **D**, Figure 6 - figure supplement 1C). Notably, HNF4*α* and p-S133-CREB1 bind to multiple subregions of ieCTNNB1 and ieCtnnb1, as well as the promoters of *CTNNB1* and *Ctnnb1* (*pCTNNB1* and *pCtnnb1*) in HCT-15 cells and small intestinal crypts (**Figure. 6C** and **D**, Figure 6 - figure supplement 1C and D). By analyzing the GEIPA-COAD (colon adenocarcinoma) and READ (rectum adenocarcinoma) database, expression levels of *CREB1* and *HNF4A* were found to be significantly higher in colon and rectum cancer samples than those of normal tissues (**Figure. 6E**). Furthermore, expression levels of *CREB1* and *HNF4A* positively correlated with that of *CTNNB1* (**Figure. 6F**). HNF4*α* and p-S133-CREB1 were significantly enriched at the promoter of *Ctnnb1* in *Apc* mutation induced colon cancer tissues (**Figure. 6G** and **H**). Intriguingly, knockout of ieCtnnb1 greatly diminished the association of HNF4*α* and p-S133-CREB1 with *Ctnnb1*'s promoter (**Figure. 6G** and **H**). In summary, HNF4*α* and p-S133-CREB1 were identified as essential trans-factors that bind to ieCTNNB1 and maintain *CTNNB1*'s expression.

Discussion

The intestinal epithelia replenish themselves rapidly throughout lifetime, which enables regeneration while predisposes to GI cancers (Clevers, 2013). The optimal strength and dynamics of canonical Wnt/β-catenin signaling is central to both homeostasis and tumorigenesis of GI tracts (Pinto et al., 2003; Silvia Maretto, 2003; Beumer & Clevers, 2016). While the stabilization and nuclear translocation of β-catenin is the key step for Wnt signaling activation, the transcriptional control of *Ctnnb1* could be another layer of regulation (Zhang & Wang, 2020; Rim et al., 2022). Here we unveiled an enhancer-dependent transcriptional machinery that tunes expressions of *Ctnnb1* in multiple cell types of intestinal crypts, thereby balancing homeostasis and tumorigenesis of intestinal epithelia (Figure supplement 8).

Our findings reinforce the notion that the canonical Wnt signaling is required for the establishment of the secretory cell lineage (Pinto et al., 2003; van Es et al., 2005; Pinto & Clevers, 2005). Expression levels of markers for secretory cells were greatly reduced whereas levels of markers for absorptive cells were elevated in all small intestinal crypt cells of $Ctnnb1^{\Delta i.enh}$ mice. Fate determinations of CBC daughter cells occur upon leaving the stem cell niche, exposed to changing WNT, Notch and EGF levels. Progenitors losing contact with PC Notch ligands upregulate DLL1 and DLL4, commit to the secretory lineage, and induce Notch activity in neighboring cells, promoting enterocyte differentiation (van Es et al., 2012; Beumer & Clevers, 2020).

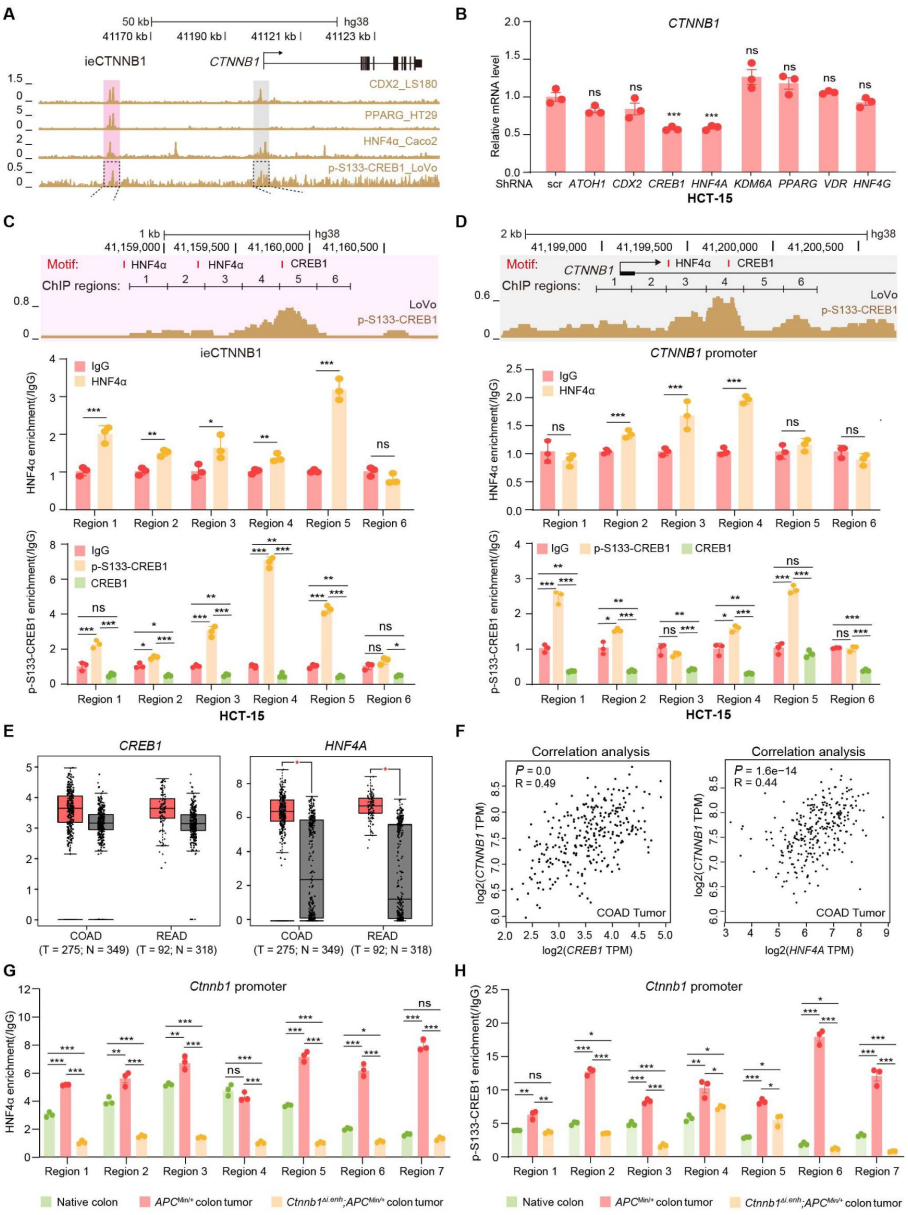

Figure 6.

HNF4α and p-S133-CREB1 associate with ieCTNNB1 to regulate *CTNNB1*'s transcription.

(A) ChIP-seq tracks of indicated trans-acting factors enriched at ieCTNNB1 (pink shading) and *CTNNB1* promoter (grey shading) in indicated colorectal cancer cell lines. Shaded regions were enlarged in C (pink) and D (grey) respectively. (B) RT-qPCR showing relative mRNA levels of *CTNNB1* in HCT-15 cells transfected with indicated shRNA-expressing plasmids for 48 hours. The expression level of *CTNNB1* in cells transfected with scramble (scr) shRNA was set to '1'. (C-D) Top: schematic diagram showing the enrichment of p-S133-CREB1 at ieCTNNB1 (C) and *CTNNB1*'s promoter (D). Locations of HNF4α and CREB1 binding motif sites were indicated. Middle and bottom: ChIP-qPCR showing enrichment of HNF4α (middle), CREB1 and p-S133-CREB1 (bottom) at ieCTNNB1 (C) and *CTNNB1*'s promoter (D) in HCT-15 cells. Locations of ChIP regions were indicated. (E) Comparison of expression levels of *CREB1* and *HNF4A* between native and tumor tissues in colon adenocarcinoma (COAD) and rectum adenocarcinoma (READ) tumors. (F) Correlations between the expression level of *CTNNB1* and those of *CREB1* or *HNF4A* in COAD tumors. (G-H) ChIP-qPCR showing enrichment of HNF4α and p-S133-CREB1 (H) at *Ctnnb1* promoter in native colon tissues of WT (n= 3) mice, tumor tissues of $Apc^{Min/+}$ (n= 3) mice and $Ctnnb1^{\Delta i.enh};Apc^{Min/+}$ (n= 3) mice. Quantification data are shown as means ± SEM, statistical significance was determined using one-way ANOVA analysis (B), unpaired two-tailed Student's *t*-test (E and F) and Multiple *t*-tests - one per row (C, D, G and H). *P < 0.05, **P < 0.01, ***P < 0.001, and ****P < 0.0001. ns, not significant. R: Pearson correlation.

WNT signaling not only directs PC-fated progenitors toward the crypt bottom but also directly induces their differentiation (van Es et al., 2005; Andreu et al., 2008; Beumer & Clevers, 2020). Single-cell sequencing and reporter gene analyses indicated that the activity of ieCtnnb1 is present in PCs. Knockout of ieCtnnb1 decreases number of PCs by almost 50% but the pool size of CBCs was not significantly altered. A previous study showed that genetic removal of PCs leads to the concomitant loss of Lgr5+ stem cells (Sato et al., 2011), while other studies indicated that PCs are not mandatory niche cells for the intestinal epithelia (Garabedian et al., 1997; Durand et al., 2012; Kim et al., 2012). Although Wnt ligands provided by PCs may support Lgr5+ CBCs[32], essential Wnt ligands are primarily supplied by subepithelial stromal populations (Degirmenci et al., 2018; Shoshkes-Carmel et al., 2018). The presence of redundancy at the stem cell niche enhances the accuracy in maintaining intestinal homeostasis.

ieCtnnb1 knockout compromises Wnt signaling dosage, leading to PC loss, dysregulation of genes controlling absorptive and secretory functions of intestinal epithelia, and reduced proliferation of stem cells. These combined effects could account for the lighter body weight observed in adult *Ctnnb1*$^{\Delta i.enh}$ mice.

On the other hand, colon and small intestinal tumors were rarely observed in *Ctnnb1*$^{\Delta i.enh}$;*Apc*$^{Min/+}$ mice. Among the few *Ctnnb1*$^{\Delta i.enh}$ tumors analyzed, they exhibited lower *Ctnnb1* expression, reduced proliferation, and behaved more like normal intestinal epithelia. Different truncations or mutations of *APC* lead to specific tumor types throughout the body in a Wnt/β-catenin dosage-dependent manner. For example, although *Apc*^{1638N};*Ctnnb1*$^{+/-}$ mice were less prone to GI cancers, *Apc*^{1638N};*Ctnnb1*$^{+/-}$ female animals tended to grow breast cancers (Bakker et al., 2013). Therefore, the intestinal specificity of ieCtnnb1 makes it an ideal target to lower the strength of Wnt signaling in treating colorectal cancer without affecting other tissues (Hamdan & Johnsen, 2019; Orouji, 2022). Importantly, ieCTNNB1 displayed higher enhancer activity in most CRC samples collected in the study. Moreover, the SNP rs15981379 (C>T) within ieCTNNB1 is associated with the expression of CTNNB1 in the GI tract. Future population studies could investigate how the enhancer activity of ieCTNNB1 and this particular SNP are associated with CRC susceptibility and prognosis.

We noticed that after knocking out ieCtnnb1, the level of β-catenin in the nuclei of small intestinal crypt cells of *Ctnnb1*$^{\Delta i.enh}$ mice decreased more significantly compared to that in the cytoplasm (49.5% vs. 29.8%). Although the loss of ieCtnnb1 should not directly lead to reduced nuclear translocation of β-catenin, RNA-seq results showed that the loss of ieCtnnb1 causes a reduction in the expression of *Bambi* (BMP and activin membrane-bound inhibitor), a target gene in the canonical Wnt signaling pathway (**Figure 1M**). BAMBI promotes the binding of Frizzled to Dishevelled, thereby stabilizing β-catenin and facilitating its nuclear translocation (Lin et al., 2008; Liu et al., 2014; Mai et al., 2014; Zhang et al., 2015). Thus, it is likely that the decreased level of BAMBI resulting from the loss of ieCtnnb1 further reduced nuclear β-catenin.

Both mouse ieCtnnb1 and human ieCTNNB1 were able to drive reporter gene expression at the base of small intestinal crypts and throughout the epithelium of the large intestine. Very intriguingly, unlike the highly conserved neCtnnb1 sequence among amniotes, mouse ieCtnnb1 and human ieCTNNB1 do not share significant homology in primary sequence (Wang et al., 2022). Nonetheless, both ieCtnnb1 and ieCTNNB1 localize at the intergenic region 30-40 kb upstream of *Ctnnb1*'s promoter. Moreover, both ieCtnnb1 and ieCTNNB1 contain binding motifs for HNF4*α* and CREB1. HNF4*α* and p-S133-CREB1 were found to associate with ieCtnnb1 and *Ctnnb1*'s promoter to maintain *Ctnnb1*'s expression. These findings support the notion that conserved TF binding motifs stabilize and preserve enhancer functionality over evolution (Zabidi & Stark, 2016; Wong et al., 2020). Of note, ieCtnnb1 and ieCTNNB1 contain distinct TF binding motifs, which may respectively exert species-specific roles in regulating the transcription of *Ctnnb1*/*CTNNB1* (Figure 6 - figure supplement 1E). Future studies will dissect common and distinct features of motif composition, location, order, and affinity with trans-factors within ieCtnnb1 and

ieCTNNB1. This analysis will provide insights how sequence variations of ieCtnnb1 are adapted to intestinal homeostasis of different species. Finally, it would be intriguing to explore how neocortical and intestinal enhancers of *Ctnnb1* controls tissue- and stage-specific transcription, as well as the existence of other potential enhancers of *Ctnnb1*.

Methods

Mice and genotyping

All animal procedures were approved by the Animal Care and Ethical Committee of Medical Research Institute at Wuhan University. C57BL/6 back-ground mice were housed in a temperature- and humidity-controlled environment with 12-hr light/dark cycle and food/water ad libitum. $Ctnnb1^{\Delta i.enh}$ mice were generated in the Beijing Biocytogen. $H11^{i.enh}$ reporter mice were generated in the Shanghai Model Organisms Center Inc. BAT-Gal mice were provided by Dr. Jun-Lei Chang (Jackson Lab, stock number 005317). *Lgr5*-EGFP-IRES-CreERT2 mice were gifts from Dr. Ye-Guang Chen (Jackson Lab, stock number 008875). $APC^{Min/+}$ mice were gifts from Dr. Bo Zhong (Jackson Lab, stock number 002020). The primer set forward 5'-atcctctgcatggtcaggtc-3'/reverse 5'-cgtggcctgattcattcc-3' was used for genotyping of BAT-Gal mice, $H11^{i.enh}$ mice and $H11^{hi.enh}$ mice with a band size of 315 base pairs (bp). The primer set forward 5'-gtcctgtccgtcactattatcctggc-3'/reverse5'-ccactgccctgctaaagcattggt-3'/reverse 5'-tgattagttctccgggaagcccagt-3' were used for genotyping of $Ctnnb1^{\Delta i.enh}$ mice and band sizes for $Ctnnb1^{\Delta i.enh}$ mice are 482 bp (wild-type allele) and 867 bp (ieCtnnb1 knockout allele). The primer set forward *5'-atctcatggcaaacagacct-3'/reverse5'-tcacaaatcatctcgcaga-3'* was used for genotyping of $APC^{Min/+}$ mice with a band size of 340 bp. The primer set *forward 5'-ctgctctctgctcccagtct-3'/reverse5'-ataccccatccctttgagc-3'/reverse 5'-gaacttcagggtcagcttgc-3'* were used for genotyping of *Lgr5*-EGFP-IRES-creERT2 mice and the band sizes for 386 bp (wild-type allele) and 119 bp (mutant allele).

Cell lines

HEK293T cells were gifts from Dr. Hong-Bing Shu (Wuhan University). HCT116, HCT-15 and HeLa cells were purchased from the China Center for Type Culture Collection. HEK293T, HeLa and HCT116 cells were grown in DMEM (Gibco) supplemented with 10% fetal bovine serum (FBS) (Life Technologies) and 1×penicillin/streptomycin (Gibco). HCT-15 cells were maintained in RPMI-1640 (Gibco) containing 10% FBS (Life Technologies) and 1×penicillin/streptomycin (Gibco). For routine culturing, cells were dissociated using 0.25% trypsin (Gibco).

Tissue fixation and section

Intestinal and tumor tissues were dissected and cleaned in pre-cooled phosphate buffered saline (PBS) and immersed in 4% paraformaldehyde (PFA) overnight at 4°C. For sectioning, intestines were embedded in Tissue-Tek® O.C.T. Compound (SAKURA) and cut to 8 μm thickness with a cryostat (Leica CM1950).

CRISPR/dCas9-mediated transcription activation (CRISPRa) and interference (CRISPRi) assay

CRISPRa and CRISPRi assay were performed as previously described (Wang et al., 2022). In brief, SgRNAs were designed using online tool (*https://zlab.bio/guide-design-resources*) and were listed in Table S2. SgRNAs were cloned into lenti sgRNA (MS2)_zeo backbone vector (Addgene, #61427).

For CRISPRi assays, pHR-SFFV-dCas9-BFP-KRAB (Addgene, #46911) is used. For CRISPRa assays, lenti MS2-P65-HSF1_Hygro (Addgene, #61426) and dCAS9-VP64_GFP (Addgene, #61422) were used. To obtain lentiviral particles, HEK293T cells (5×10^6 cells per 10-cm dish) were transiently transfected with 12 μg CRISPRa or CRISPRi constructs, 6 μg psPAX2 and 6 μg pMD2.G. The

supernatant containing lentivirus particles was harvested at 72 hours after transfection and filtered through Millex-GP Filter Unit (0.45 μm pore size, Millipore). To obtain high virus titer, the supernatant was centrifuged at 10,000×*g* for 100 minutes and concentrate to 100 μl. On the day before infection, HCT-15 cells (2×10^5 cells per well) were inoculated in 12 well plates. 10 μl high titer viruses were added to each well. 72 hours after infection, cells were harvested for RT-qPCR analysis.

RNA isolation and cDNA synthesis

RNAiso Plus (TAKARA) is used for RNA isolation. 1 ml RNAiso Plus was added to DNase/RNase free EP tube to lyse tissues or cells, followed by adding one-fifth volume of chloroform to achieve phase separation. After vigorous shaking, centrifuge at 12,000×*g* for 15 minutes at 4°C. The upper aqueous phase was transferred to a new DNase/RNase free EP tube and equal volume of isopropanol was added to precipitate RNA. Precipitation was dissolved in DNase/RNase-free water. Complementary DNAs (cDNAs) were synthesized by HiScript® II Q RT SuperMix for qPCR kit (Vazyme; R222-01).

Real-time quantitative reverse transcription PCR (RT-qPCR)

cDNA was subjected to RT-qPCR using the SYBR Green assay with 2× SYBR Green qPCR master mix (Bimake). PCR reactions were performed on a CFX Connect Real-Time PCR Detection System (Bio-rad) under the following condition: 5 minutes at 95°C, 40 cycles at 95°C for 15 seconds, 60°C for 20 seconds. The relative transcript level of each gene was normalized to *Gapdh* (mice) or *ACTB* (human) and calculated according to the $2^{-\Delta\Delta Ct}$ method. All primers used are shown in the Table S2.

Isolation of murine intestinal crypt cells

Murine small intestines were harvested and cut open longitudinally. After 3 times wash in cold PBS with Penicillin (200 U/ml) + Streptomycin (200 μg/ml) (Invitrogen), small intestines were cut into 5 cm segments and incubated in pre-cold PBS with 8 mM EDTA at 4°C for 2 hours. Then intestinal tissues were transferred into a centrifuge tube filled with new cold PBS. Shake vigorously for 5 minutes and collect intestinal epithelial cells (villi plus crypts) from the supernatant. Centrifuge the supernatant to collect all epithelial cells or pass through 70 μm cell filter (Corning) to filter out villi. Crypts were spun down in a centrifuge at 300×*g* for 5 minutes.

Enriching *Lgr5*-EGFP$^+$ cells

Crypts were collected from *Lgr5*-EGFP and *H11*$^{i.enh.}$;*Lgr5*-EGFP mice, followed by resuspension and single-cell digestion in DMEM containing 0.25% trypsin (Gibco) at 37°C for 5 minutes. Disaggregated cells were passed through 40 μm cell strainers (Corning). *Lgr5*-EGFP$^+$ and *Lgr5*-EGFP$^-$ cells were collected using a BD Arial III cell sorter.

X-Gal staining

X-Gal staining is performed as described (Wang et al., 2022). In short, frozen slides were placed in fixed buffer (0.2% PFA, 0.1 M PIPES buffer (pH 6.9), 2 mM MgCl2, 5 mM EGTA) for 10 minutes, followed by rinse for two times with PBS containing 2 mM $MgCl_2$. Then slides were incubated with detergent solution (0.1 M PBS (pH 7.3), 2 mM MgCl2, 0.01% sodium deoxycholate, 0.02% Nonidet P-40) for 10 minutes. Slides were incubated with freshly prepared and filtered X-Gal staining solution (0.1 M PBS (pH 7.3), 2 mM MgCl2, 0.01% sodium-deoxycholate, 0.02% Nonidet P-40, 5 mM $K_3Fe(CN)_6$, 5 mM $K_4Fe(CN)_6 \cdot 3H_2O$ and 1 mg/ml X-Gal) overnight in the dark at 37°C. For whole gastrointestinal tissues, tissues were fixed in freshly prepared 4% PFA for 10 minutes, followed by rinse with detergent solution for 5 minutes by three times. Tissues were incubated with freshly prepared and filtered X-Gal staining solution at 37°C for a few hours.

EdU pulse-labeling experiment

Mice were intraperitoneally injected with EdU (10 mg/kg of body weight). After 4 hours, harvest the intestines for frozen sectioning. Staining was performed using BeyoClick^{TM} EdU Cell Promotion Kit (C0075S, Beyotime, China) according to the manufacturer's manual.

ChIP-qPCR assay

Cells were cross-linked with 1% formaldehyde for 10 minutes at room temperature and then quenched with 0.125 M glycine for 5 minutes and washed twice with cold PBS. Cells were resuspended with 500 µl lysis buffer (50 mM Tris-HCl, pH 8.0, 0.5% SDS, 5 mM EDTA) and subjected to sonication on ice with an output power of 100 W, 12 minutes, 0.5 seconds on, 0.5 seconds off. After centrifugation, 1% of the supernatant was taken out as input. The DNA fragment lengths were measured by gel electrophoresis, showing fragments between 200 bp and 500 bp, with an average length around 300 bp. The rest of the sonicated lysates was diluted into 0.1% SDS and divided into several equal parts. Immunoprecipitation was performed overnight at 4°C on a rotating wheel with sheared chromatin, protein G agarose beads and indicated antibodies: 2 µg HNF4*α* (Abcam, ab181604), 2 µg p-S133-CREB1 (Abcam, ab32096), 2 µg IgG antibody (ABclonal, AC005). The next day, beads were cleaned three times with Wash Buffer I (20 mM Tris-HCl, pH 8.0; 1% Triton X-100; 2 mM EDTA; 150 mM NaCl; 0.1% SDS), Wash Buffer II (20 mM Tris-HCl, pH 8.0; 1% Triton X-100; 2 mM EDTA; 500 mM NaCl; 0.1% SDS), Wash Buffer III (10 mM Tris-HCl, pH 8.0; 1 mM EDTA; 0.25 M LiCl; 1% NP-40; 1% deoxycholate) and TE buffer. Protein-DNA complexes were de-crosslinked in 120 µl elution buffer (0.1 M $NaHCO_3$, 1% SDS, 20 µg/ml proteinase K) and shaken at 65°C overnight. DNA purification kit (TIANGEN) was used to extract DNA fragments for qPCR.

The efficiency of qPCR primers was evaluated using gradient diluted (10^0, 10^{-1}, 10^{-2}, 10^{-3}, 10^{-4}, 10^{-5}) of mouse or human genomes as templates. After completing qPCR reaction, the dilution factors were plotted on the X-axis using log10 values, and the corresponding Ct value were plotted on the Y-axis to create a standard curve. The equation y = kx + b was derived, and the primer efficiency was calculated using the formula E = 10^(−1/k) - 1. The results indicated that the primer efficiency ranged from 90% to 110%, with no significant differences observed.

Luciferase reporter assay

The luciferase reporter assay was performed as described previously (Li et al., 2017). Briefly, the core region of ieCtnnb1, 5 regions of ieCTNNB1 and the region containing the mutation site were respectively cloned into pGL3-promoter vector (Promega). HEK293T, HeLa and HCT116 cells were transfected with pGL3-promoter vector and the plasmids mentioned above. *Renilla* basic vector was co-transfected as a control for normalization of luciferase activity. After 48 hours of transfection, Promega Dual Glo test kit (Promega, E1910) was used to measure luciferase activity according to manufacturer's instructions.

Immunohistochemical staining

Frozen sections were dried at 37°C, fixed with 4% PFA for 10 minutes, and then washed three times with PBS. Antigen retrieval was performed using citrate buffer (pH 6, epitope retrieval solution) at 95°C for 20 minutes. Slides were then placed in 3% H_2O_2 solution for a few hours to remove endogenous catalase. After washing with PBS three times, slides were blocked with 10% normal goat serum for 1 hour, then incubated with the following primary antibodies overnight at 4°C: rabbit anti-α-defensin5 (Abcam, ab80515, 1:500), rabbit anti-Ki67 (Abcam, ab15580, 1:500), rabbit anti-β-catenin (Cell Signaling Technology, 8480T, 1:100), rabbit anti-Muc2 (Thermo Fisher Scientific, PA5-21329, 1:500). The next day, slides were incubated with biotin labeled secondary antibodies at room temperature for 1 hour. Then, slides were incubated with the avidin-biotin-

peroxidase complex (VECTASTAIN Elite ABC system, Vector Labs). Finally, colorization was performed in the reaction solution (Tris-HCl (pH 7.2), 5 mg/ml 3,3'-diaminobenzidine, 0.075% H_2O_2).

H&E staining

H&E staining kit (Beyotime Biotech, C0105S) was used for experiments. Frozen slides were dried at 65°C, then dripped with hematoxylin staining solution for 5 minutes. Excess staining solution was rinsed off with water. Slides were immersed in distilled water for 5 minutes, then rinsed with 95% ethanol, and stained with eosin solution for 30 seconds. Subsequently, slides were put into anhydrous ethanol for 2 minutes, and cleared with xylene for 5 minutes. After air dry, slides were sealed with neutral resin.

Immunoblotting analysis

Crypt cells were lysed by 1× SDS loading buffer at 95°C for 10 minutes. After short centrifugation, the supernatants were loaded onto 10% SDS-polyacrylamide gel electrophoresis gels. Then, proteins were transferred onto polyvinylidene fluoride membrane (Millipore). Membranes were blocked with 10% non-fat milk in tris-buffered saline containing 0.3% Tween 20 (TBST; pH 7.4) for 1 hour at room temperature. Immunoblotting was carried out used primary antibody: rabbit anti-β-catenin (Cell Signaling Technology, 8480T, 1:100); mouse anti-GAPDH (ABclonal, AC001, 1:1000); rabbit anti-H3 (ABclonal, A2348, 1:10,000). After three times of washing with TBST, the membrane was incubated with anti-rabbit immunoglobulin G (IgG)–conjugated horseradish peroxidase secondary for 1 hour at room temperature. Signals were detected using the ECL substrate (Thermo Fisher Scientific).

Alcian Blue PAS Staining

Alcian Blue PAS Stain Kit (Abcam, ab245876) was used for experiments. all materials and prepared reagents were equilibrated to room temperature and gently agitated prior to use. Tissue sections were applied with acetic acid solution (3%) for 2 minutes. Then alcian blue solution (pH 2.5) was applied for 15-20 minutes. Slides were rinsed with running tap water for 2 minutes followed by 2 changes of distilled water. Periodic acid solution was applied to tissue sections for 5 minutes. After slides were rinsed with two changes of distilled water, Schiff's solution was applied to tissue sections for 10-20 minutes. Slides were rinsed with warm running tap water for 2 minutes followed by 2 changes of distilled water. Tissue sections were applied with hematoxylin for 2 minutes. Sections were rinsed in running tap water for 2 minutes followed by 2 changes of distilled water. Slides were dehydrated through graded alcohols and sealed with synthetic resin.

Cell Sorting

Crypt single cells were prepared as described above. Enrichment of epithelial cells by cell sorting was carried out according to reported protocols with slight modification (Haber et al., 2017; Huang et al., 2022). Cells were resuspended using 1 ml PBS and stained with 5 μl anti-EpCAM-FITC (eBioScience, 11-5791-82) at 4°C for 30 minutes. After washing with PBS three times, cells were resuspended using 1 M FACS buffer (PBS with 1%BSA) containing 0.2 μg/ml DAPI (BD Pharmingen, Cat. No. 564907). Cells were filtered with nylon membrane with a 40 μm pore size. EpCAM positive cells were sorted and collected based on fluorescence signals for subsequent single cell sequencing. Flow cytometry data were acquired on a BD Arial III flow cytometer and analyzed with FlowJo (version 10.6.2).

Bulk RNA sequencing

RNA-seq and data analyses were performed at Novogene Co., Ltd (Beijing, China). Crypt cells or tumor tissues were harvested and total RNAs were extracted. RNA integrity was assessed using the RNA Nano 6000 Assay Kit of the Bioanalyzer 2100 system (Agilent Technologies, CA, USA). RNA-seq

library construction was performed as described previously (Xu et al., 2021). Briefly, first strand cDNA was synthesized using random hexamer primer and M-MuLV Reverse Transcriptase (RNase H-). Second strand cDNA synthesis was subsequently performed using DNA Polymerase I and RNase H. Then, the library fragments were purified with AMPure XP system (Beckman Coulter, Beverly, USA). Then PCR was performed with Phusion High-Fidelity DNA polymerase, Universal PCR primers and Index (X) Primer. At last, PCR products were purified (AMPure XP system). The clustering of the index-coded samples was performed on a cBot Cluster Generation System using TruSeq PE Cluster Kit v3-cBot-HS (Illumia) according to the manufacturer's instructions. After cluster generation, the library preparations were sequenced on an Illumina Novaseq platform and 150 bp paired-end reads were generated.

Bulk RNA-seq data processing

For data analysis, raw data of fastq format were firstly processed through in-house perl scripts. In this step, clean data were obtained by removing reads containing adapter, reads containing poly-N (indicating bases that were not detected and hence signal-free), and low-quality reads from the raw data. Index of the reference genome was built using Hisat2 v2.0.5 and paired-end clean reads were aligned to the reference genome using Hisat2 v2.0.5. featureCounts v1.5.0-p3 was used to count reads numbers mapped to each gene. Differential expression analysis of two groups was performed using the DESeq2 R package (1.20.0). The resulting P-values were adjusted using the Benjamini and Hochberg's approach for controlling the false discovery rate. Genes with an adjusted P-value <0.05 found by DESeq2 were assigned as differentially expressed. Gene Ontology (GO) enrichment analysis of differentially expressed genes was implemented by the clusterProfiler R package, in which gene length bias was corrected. clusterProfiler R package was also used to test the statistical enrichment of differential expression genes in KEGG pathways. Local version of the GSEA analysis tool (*http://www.broadinstitute.org/gsea/index.jsp*), GO、KEGG、Reactome、DO and DisGeNET data sets were used for GSEA independently.

Single-Cell RNA sequencing and data analysis

ScRNA-seq and data analysis were performed at Novogene Co., Ltd (Beijing, China). The protoplast suspension was loaded into Chromium microfluidic chips with 30 chemistry (v2 or v3) and barcoded with a 10× Chromium Controller (10X Genomics). RNA from the barcoded cells was subsequently reverse-transcribed and sequencing libraries constructed with reagents from a Chromium Single Cell 30 v2 reagent kit (10X Genomics) according to the manufacturer's instructions. Sequencing was performed with Illumina HiSeq 2000 according to the manufacturer's instructions. For data analysis, we use FastQC to perform basic statistics on the quality of the raw reads. Raw reads were demultiplexed and mapped to the reference genome by 10X Genomics Cell Ranger pipeline using default parameters. All downstream single-cell analyses were performed using Cell Ranger and Seurat unless mentioned specifically. In brief, for each gene and each cell barcode (filtered by CellRanger), unique molecule identifiers were counted to construct digital expression matrices. Secondary filtration by Seurat: a gene with expression in more than 3 cells was considered as expressed, and each cell was required to have at least 200 expressed genes.

Hi-C data analysis

Hi-C data analysis completed by Frasergen Medicine Co., Ltd (Wuhan, China). Hi-C data of BALB/c mice large intestinal epithelial cells were provided by Dr. Gen Zheng (Zheng et al., 2023). The Hi-C data of SW480 cells was obtained from deposited data (Orouji, 2022). According to the reported method, the dynamic changes of TAD structures can be explored by calculating the relative signal values of TAD boundaries. TAD boundaries that are common among individuals and are not within the 2 Mb range of chromosomal ends were included, followed by filtering out boundaries with interactions less than 10 in the 2 Mb upstream and downstream regions. The ratio of the interaction between the boundary and its 2 Mb upstream and downstream regions

were calculated using log2 to obtain the signal value of the TAD boundary, then the minimum value was subtracted from it to finally obtain the distribution of the relative signal value of each sample TAD boundary.

ChIP-seq data analysis

The human colorectal cancer patient RNA-seq FPKM files and ChIP-seq data were from GEO dataset GSE156614 (Q. L. Li et al., 2021). All ChIP-seq raw fastq data were removed of adaptor sequence. Cutadapt (version 1.16) was used with the parameters -u 3 -u −10 -U 3 -U −10 -m 30. Cleaned reads were aligned to the human reference genome (hg19) using bowtie2 (version 2.4.4) with default settings. The CrossMap (0.6.5) package was used as a conversion between different versions of the human genome (hg19 and hg38). We calculated the normalized RPM (reads per million mapped reads) of ChIP-seq signal at ieCTNNB1 and *CTNNB1* promoter. Briefly, reads aligned to the specified region were calculated with bedtools multicov command. These reads were normalized with RPM. RNA-seq data FPKM (Reads per kilobase per million mapped reads) were converted to TPM (Transcript per Kilobase per Million mapped reads) using R version 4.2.3.

Knockdown experiments

Target sequences for shRNAs were designed on the Merck Life Sciences website (*https://www.sigmaaldrich.cn*) and were listed in Table S2. Oligonucleotides for shRNAs were cloned into pLKO.1 vector (Addgene, #21297). The day before transfection, HEK293T cells (2×10^5 cells per well) were seeded in 12-well plates. pLKO.1 constructs, psPAX2 and pMD2.G were co-transfected into HEK293T cells. After 72 hours, supernatant containing virus particles was harvested and passed through Millex-GP Filter Unit (0.45 μm pore size, Millipore). Viral particles were aliquoted and stored at −80°C. On the day before infection, HCT-15 cells (2×10^5 cells per well) were seeded in 12-well plates. 20 μl virus suspension were added to each well. After 72 hours, cells were harvested for RT-qPCR to evalutate knockdown efficiency.

Reference database

ChIP-seq signals for H3K27ac, H3K4me3, H3K4me1, H3K36me3, and DNase I hypersensitivity data of stomach, intestines, liver, and other tissues at different stages were downloaded from the ENCODE (*https://www.encodeproject.org/*) and their identifiers are listed in Table S1. In addition, ChIP-seq data for listed transcription factors of cells or tissues were obtained from Cistrome Data Browser (*http://cistrome.org*). Expressions of *HNF4A* and *CREB1* in human colon (COAD) and rectal (READ) cancers were obtained from GEPIA (gepia.cancer-pku.cn).

eQTL analysis

The GTEX database (*https://www.gtexportal.org/home/*) was used to search SNPs at *CTNNB1* and the 1 MB upstream and downstream region, followed by eQTL analysis. A variant, rs115981379 (C>T), was identified inside *CTNNB1*. The expression levels of *CTNNB1* in 428 C/C type and 37 C/T type esophagus samples, and 343 C/C type and 25 C/T type transverse colon samples were also obtained in the GTEX database.

Analyses of HNF4*α* and CREB1 binding motifs

The JASPAR database (*https://jaspar.elixir.no/*) was used to analyze binding motifs of HNF4*α* and CREB1 at ieCtnnb1/ieCTNNB1 and *Ctnnb1/CTNNB1* promoter. Results are listed in Table S3.

Nuclear-cytoplasmic separation

Nuclear and cytoplasmic protein extraction kit (Beyotime Biotech, P0027) was used for experiments. Small intestinal crypts were collected from wild-type and $Ctnnb1^{\Delta i.enh}$ mice as described above. According to manufacturer's instructions, 20 μl cell precipitation was resuspended in 200 μl cytoplasmic protein extraction reagent A with 1 mM PMSF. After placing on

ice for 15 minutes, 10 µl cytoplasmic protein extraction reagent B was added. After vigorous vortex, solutions were centrifuged at 12,000×*g* for 5 minutes at 4°C. The supernatant was collected as the extracted cytoplasmic protein. The precipitate was resuspended with 50 µl nuclear protein extraction reagent with 1 mM PMSF. Solutions were placed on ice and vortex vigorously every 2 minutes for a total of 30 minutes. After centrifuging at 12,000×*g* for 10 minutes at 4°C, the supernatant was collected as the extracted nuclear protein.

Statistics

All experiments reported in this study were repeated at least three independent times. *In vivo* analyses were conducted with at least three animals per condition. The number of animals in each experiment is depicted in Figure legends. The signal intensity of tumor stain region was generated using ImageJ software (version 6.0.0.260) as described previously (Wang et al., 2021). GraphPad Prism (version 8.0.2) was used to determine statistical significance. Unpaired two-tailed Student's t-test were used for analysis between two groups of equal variances by *F*-tests. When the *F*-test of equal variance failed, the Welch *t*-tests were used. Data comparison of three or more groups with control groups were analyzed using one-way ANOVA followed by Dunnett's multiple comparison test.

Data comparison of three or more groups among each other were analyzed using one-way ANOVA followed by Tukey's multiple comparison test. The exact *P* values were reported in each figure or indicated as ****, $P < 0.0001$; ***, $P < 0.001$; **, $P < 0.01$; *, $P < 0.05$, ns = not significant.

Data and code availability

The GEO accession number for the bulk RNA-seq and scRNA-seq data reported in this paper is GSE233979. RNA-seq data of mouse small intestinal crypt and colon tumor have been deposited at GEO: GSE233977. ScRNA-seq data of mouse small intestinal crypt cells in this study have been deposited at GEO: GSE233978. All data are publicly available as of the date of publication. Custom codes were described in detail at methods part. Any additional information required to analyze the data in this paper is available from authors upon reasonable request.

Acknowledgements

We thank Dr. Yeguang Chen for providing the *Lgr5*-EGFP-IRES-CreERT2 mice. We thank the Core Facility and the Animal Facility of Medical Research Institute of Wuhan University for technical support. We thank all Zhou lab members for critical reading of the manuscript. Y. Zhou was supported by grants from National Key R&D Program of China (2022YFA0806603 and 2018YFA0800700), National Natural Science Foundation of China (32270876 and 31970770), and the Fundamental Research Funds for the Central Universities (2042022dx0003 and 2042023kf0234). Y.L. was supported by grants from National Key R&D Program of China (2018YFA0800700 and 2022YFA0806603), National Natural Science Foundation of China (31970676), and Hubei Natural Science Foundation (2022CFB128).

Author contributions

Y.Z. conceived and designed the study; X.H. and J.W. performed experiments and analyzed data; C.Z. assisted with processing ChIP-seq data; J.T. and X.P. retrieved and analyzed eQTL data. M.Y. and M.W. provided RNA-seq and ChIP-seq data of colorectal cancer samples; G.Z. provided Hi-C

data; Y.Z. and X.H. wrote the paper. Y.Z. and Y.L. provided funding and supervised the study. All authors discussed results and commented to the manuscript.

Competing interests

The authors claimed that they have no competing interests.

References

Andreu P., Peignon G., Slomianny C., Taketo M. M., Colnot S., Robine S., Lamarque D., Laurent-Puig P., Perret C., Romagnolo B (2008) **A genetic study of the role of the Wnt/beta-catenin signalling in Paneth cell differentiation** *Dev Biol* **324**:288–296 https://doi.org/10.1016/j.ydbio.2008.09.027

Ayyaz A. *et al.* (2019) **Single-cell transcriptomes of the regenerating intestine reveal a revival stem cell** *Nature* **569**:121–125 https://doi.org/10.1038/s41586-019-1154-y

Bakker E. R., Hoekstra E., Franken P. F., Helvensteijn W., van Deurzen C. H., van Veelen W., Kuipers E. J., Smits R. (2013) **. beta-Catenin signaling dosage dictates tissue-specific tumor predisposition in Apc-driven cancer** *Oncogene* **32**:4579–4585 https://doi.org/10.1038/onc.2012.449

Barker N. *et al.* (2007) **Identification of stem cells in small intestine and colon by marker gene Lgr5** *Nature* **449**:1003–1007 https://doi.org/10.1038/nature06196

Barreto E. B. L., Rattes I. C., da Costa A. V., Gama P. (2022) **Paneth cells and their multiple functions** *Cell Biol Int* **46**:701–710 https://doi.org/10.1002/cbin.11764

Beumer J., Clevers H (2016) **Regulation and plasticity of intestinal stem cells during homeostasis and regeneration** *Development* **143**:3639–3649 https://doi.org/10.1242/dev.133132

Beumer J., Clevers H (2020) **Cell fate specification and differentiation in the adult mammalian intestine** *Nature Reviews Molecular Cell Biology* **22**:39–53 https://doi.org/10.1038/s41580-020-0278-0

Carlezon W. A., Duman R. S., Nestler E. J (2005) **The many faces of CREB** *Trends Neurosci* **28**:436–445 https://doi.org/10.1016/j.tins.2005.06.005

Cattin A. L. *et al.* (2009) **Hepatocyte nuclear factor 4alpha, a key factor for homeostasis, cell architecture, and barrier function of the adult intestinal epithelium** *Mol Cell Biol* **29**:6294–6308 https://doi.org/10.1128/MCB.00939-09

Cheng X., Xu X., Chen D., Zhao F., Wang W (2019) **Therapeutic potential of targeting the Wnt/beta-catenin signaling pathway in colorectal cancer** *Biomed Pharmacother* **110**:473–481 https://doi.org/10.1016/j.biopha.2018.11.082

Chin A. M., Hill D. R., Aurora M., Spence J. R (2017) **Morphogenesis and maturation of the embryonic and postnatal intestine** *Semin Cell Dev Biol* **66**:81–93 https://doi.org/10.1016/j.semcdb.2017.01.011

Clevers H (2006) **Wnt/beta-catenin signaling in development and disease** *Cell* **127**:469–480 https://doi.org/10.1016/j.cell.2006.10.018

Clevers H (2013) **The intestinal crypt, a prototype stem cell compartment** *Cell* **154**:274–284 https://doi.org/10.1016/j.cell.2013.07.004

Clevers H., Loh K. M., Nusse R (2014) **Stem cell signaling. An integral program for tissue renewal and regeneration: Wnt signaling and stem cell control** *Science* **346** https://doi.org/10.1126/science.1248012

Clevers H., Nusse R (2012) **Wnt/beta-catenin signaling and disease** *Cell* **149**:1192–1205 https://doi.org/10.1016/j.cell.2012.05.012

Cosmas D., Arnold D. G., Stelzer Christoph, Boryn Łukasz M., Rath Martina, Stark Alexander (2013) **Genome-Wide Quantitative Enhancer Activity Maps Identified by STARR-seq** *Science* **339**:1074–1077 https://doi.org/10.1126/science.1232542

Degirmenci B., Valenta T., Dimitrieva S., Hausmann G., Basler K (2018) **GLI1-expressing mesenchymal cells form the essential Wnt-secreting niche for colon stem cells** *Nature* **558**:449–453 https://doi.org/10.1038/s41586-018-0190-3

Durand A., Donahue B., Peignon G., Letourneur F., Cagnard N., Slomianny C., Perret C., Shroyer N. F., Romagnolo B (2012) **Functional intestinal stem cells after Paneth cell ablation induced by the loss of transcription factor Math1 (Atoh1)** *Proceedings of the National Academy of Sciences* **109**:8965–8970 https://doi.org/10.1073/pnas.1201652109

Garabedian E. M., Roberts L. J. J., McNevin M. S., Gordon J. I (1997) **Examining the Role of Paneth Cells in the Small Intestine by Lineage Ablation in Transgenic Mice** *Journal of Biological Chemistry* **272**:23729–23740 https://doi.org/10.1074/jbc.272.38.23729

Garrison W. D., Battle M. A., Yang C., Kaestner K. H., Sladek F. M., Duncan S. A (2006) **Hepatocyte nuclear factor 4alpha is essential for embryonic development of the mouse colon** *Gastroenterology* **130**:1207–1220 https://doi.org/10.1053/j.gastro.2006.01.003

Gribble F. M., Reimann F (2019) **Function and mechanisms of enteroendocrine cells and gut hormones in metabolism** *Nature Reviews Endocrinology* **15**:226–237 https://doi.org/10.1038/s41574-019-0168-8

Gu W. *et al.* (2022) **SATB2 preserves colon stem cell identity and mediates ileum-colon conversion via enhancer remodeling** *Cell Stem Cell* **29**:101–115 https://doi.org/10.1016/j.stem.2021.09.004

Gustafsson J. K., Johansson M. E. V (2022) **The role of goblet cells and mucus in intestinal homeostasis** *Nature Reviews Gastroenterology & Hepatology* **19**:785–803 https://doi.org/10.1038/s41575-022-00675-x

Haber A. L. *et al.* (2017) **A single-cell survey of the small intestinal epithelium** *Nature* **551**:333–339 https://doi.org/10.1038/nature24489

Hamdan F. H., Johnsen S. A (2019) **Perturbing Enhancer Activity in Cancer Therapy** *Cancers (Basel)* **11** https://doi.org/10.3390/cancers11050634

Huang X.-T. *et al.* (2022) **Embryogenic stem cell-derived intestinal crypt fission directs de novo crypt genesis** *Cell Reports* **41** https://doi.org/10.1016/j.celrep.2022.111796

Huels D. J. *et al.* (2018) **Wnt ligands influence tumour initiation by controlling the number of intestinal stem cells** *Nature Communications* **9** https://doi.org/10.1038/s41467-018-03426-2

Jindal G. A., Farley E. K (2021) **Enhancer grammar in development, evolution, and disease: dependencies and interplay** *Dev Cell* **56**:575–587 https://doi.org/10.1016/j.devcel.2021.02.016

Kim T.-H., Escudero S., Shivdasani R. A (2012) **Intact function of Lgr5 receptor-expressing intestinal stem cells in the absence of Paneth cells** *Proceedings of the National Academy of Sciences* **109**:3932–3937 https://doi.org/10.1073/pnas.1113890109

Krausova M., Korinek V (2014) **Wnt signaling in adult intestinal stem cells and cancer** *Cell Signal* **26**:570–579 https://doi.org/10.1016/j.cellsig.2013.11.032

Kurokawa K., Hayakawa Y., Koike K (2020) **Plasticity of Intestinal Epithelium: Stem Cell Niches and Regulatory Signals** *Int J Mol Sci* **22** https://doi.org/10.3390/ijms22010357

Kvon E. Z., Waymack R., Gad M., Wunderlich Z (2021) **Enhancer redundancy in development and disease** *Nat Rev Genet* **22**:324–336 https://doi.org/10.1038/s41576-020-00311-x

Kvon E. Z. *et al.* (2020) **Comprehensive In Vivo Interrogation Reveals Phenotypic Impact of Human Enhancer Variants** *Cell* **180**:1262–1271 https://doi.org/10.1016/j.cell.2020.02.031

Li J., Ma X., Chakravarti D., Shalapour S., DePinho R. A (2021) **Genetic and biological hallmarks of colorectal cancer** *GENES & DEVELOPMENT* **35**:787–820 https://doi.org/10.1101/gad.348226

Li Q. L. *et al.* (2021) **Genome-wide profiling in colorectal cancer identifies PHF19 and TBC1D16 as oncogenic super enhancers** *Nat Commun* **12** https://doi.org/10.1038/s41467-021-26600-5

Li Y. *et al.* (2017) **Paired related homeobox 1 transactivates dopamine D2 receptor to maintain propagation and tumorigenicity of glioma-initiating cells** *Journal of Molecular Cell Biology* **9**:302–314 https://doi.org/10.1093/jmcb/mjx017

Li Y. E. *et al.* (2021) **An atlas of gene regulatory elements in adult mouse cerebrum** *Nature* **598**:129–136 https://doi.org/10.1038/s41586-021-03604-1

Lin Z., Gao C., Ning Y., He X., Wu W., Chen Y.-G (2008) **The Pseudoreceptor BMP and Activin Membrane-bound Inhibitor Positively Modulates Wnt/β-Catenin Signaling** *Journal of Biological Chemistry* **283**:33053–33058 https://doi.org/10.1074/jbc.M804039200

Liu K. A. I., Song X., Ma H., Liu L., Wen X., Yu J., Wang L., Hu S (2014) **Knockdown of BAMBI inhibits β-catenin and transforming growth factor β to suppress metastasis of gastric cancer cells** *Molecular Medicine Reports* **10**:874–880 https://doi.org/10.3892/mmr.2014.2305

Lueschow S. R., McElroy S. J (2020) **The Paneth Cell: The Curator and Defender of the Immature Small Intestine** *Front Immunol* **11** https://doi.org/10.3389/fimmu.2020.00587

Luis Tiago C., Naber Brigitta A. E., Roozen Paul P. C., Brugman Martijn H., de Haas Edwin F. E., Ghazvini M., Fibbe Willem E., van Dongen Jacques J. M., Fodde R., Staal Frank J. T. (2011) **Canonical Wnt Signaling Regulates Hematopoiesis in a Dosage-Dependent Fashion** *Cell Stem Cell* **9**:345–356 https://doi.org/10.1016/j.stem.2011.07.017

Mah A. T., Yan K. S., Kuo C. J (2016) **Wnt pathway regulation of intestinal stem cells** *J Physiol* **594**:4837–4847 https://doi.org/10.1113/JP271754

Mai Y., Zhang Z., Yang H., Dong P., Chu G., Yang G., Sun S (2014) **BMP and activin membrane-bound inhibitor (BAMBI) inhibits the adipogenesis of porcine preadipocytes through Wnt/β-catenin signaling pathway** *Biochemistry and Cell Biology* **92**:172–182 https://doi.org/10.1139/bcb-2014-0011

Metcalfe C., Kljavin N. M., Ybarra R., de Sauvage F. J. (2014) **Lgr5+ stem cells are indispensable for radiation-induced intestinal regeneration** *Cell Stem Cell* **14**:149–159 https://doi.org/10.1016/j.stem.2013.11.008

Nakamura T., Tsuchiya K., Watanabe M (2007) **Crosstalk between Wnt and Notch signaling in intestinal epithelial cell fate decision** *J Gastroenterol* **42**:705–710 https://doi.org/10.1007/s00535-007-2087-z

Nalapareddy K. *et al.* (2017) **Canonical Wnt Signaling Ameliorates Aging of Intestinal Stem Cells** *Cell Reports* **18**:2608–2621 https://doi.org/10.1016/j.celrep.2017.02.056

Noah T. K., Donahue B., Shroyer N. F (2011) **Intestinal development and differentiation** *Exp Cell Res* **317**:2702–2710 https://doi.org/10.1016/j.yexcr.2011.09.006

Nusse R., Clevers H (2017) **Wnt/beta-Catenin Signaling, Disease, and Emerging Therapeutic Modalities** *Cell* **169**:985–999 https://doi.org/10.1016/j.cell.2017.05.016

Orouji E. *et al.* (2022) **Chromatin state dynamics confers specific therapeutic strategies in enhancer subtypes of colorectal cancer** *Gut* **71**:938–949 https://doi.org/10.1136/gutjnl-2020-322835

Pachano T., Haro E., Rada-Iglesias A (2022) **Enhancer-gene specificity in development and disease** *Development* **149** https://doi.org/10.1242/dev.186536

Pentinmikko N. *et al.* (2019) **Notum produced by Paneth cells attenuates regeneration of aged intestinal epithelium** *Nature* **571**:398–402 https://doi.org/10.1038/s41586-019-1383-0

Pinto D., Clevers H (2005) **Wnt control of stem cells and differentiation in the intestinal epithelium** *Exp Cell Res* **306**:357–363 https://doi.org/10.1016/j.yexcr.2005.02.022

Pinto D., Gregorieff A., Begthel H., Clevers H (2003) **Canonical Wnt signals are essential for homeostasis of the intestinal epithelium** *Genes Dev* **17**:1709–1713 https://doi.org/10.1101/gad.267103

Ramadan R., van Driel M. S., Vermeulen L., van Neerven S. M. (2022) **Intestinal stem cell dynamics in homeostasis and cancer** *Trends Cancer* **8**:416–425 https://doi.org/10.1016/j.trecan.2022.01.011

Rim E. Y., Clevers H., Nusse R (2022) **The Wnt Pathway: From Signaling Mechanisms to Synthetic Modulators** *Annu Rev Biochem* **91**:571–598 https://doi.org/10.1146/annurev-biochem-040320-103615

Sato T., van Es J. H., Snippert H. J., Stange D. E., Vries R. G., van den Born M., Barker N., Shroyer N. F., van de Wetering M., Clevers H. (2011) **Paneth cells constitute the niche for Lgr5 stem cells in intestinal crypts** *Nature* **469**:415–418 https://doi.org/10.1038/nature09637

Schneider C., O'Leary C. E., Locksley R. M (2019) **Regulation of immune responses by tuft cells** *Nature Reviews Immunology* **19**:584–593 https://doi.org/10.1038/s41577-019-0176-x

Sengupta S., George R. E (2017) **Super-Enhancer-Driven Transcriptional Dependencies in Cancer** *Trends Cancer* **3**:269–281 https://doi.org/10.1016/j.trecan.2017.03.006

Shoshkes-Carmel M., Wang Y. J., Wangensteen K. J., Tóth B., Kondo A., Massasa E. E., Itzkovitz S., Kaestner K. H (2018) **Subepithelial telocytes are an important source of Wnts that supports intestinal crypts** *Nature* **557**:242–246 https://doi.org/10.1038/s41586-018-0084-4

Silvia Maretto M. C., Dupont Sirio, Braghetta Paola, Vania Broccoli A. Bassim, Hassan Dino, Volpin Giorgio M., Bressan Stefano, Piccolo (2003) **Mapping Wnt/β- catenin signaling during mouse development and in colorectal tumors** *PNAS*

Snoeck V., Goddeeris B., Cox E (2005) **The role of enterocytes in the intestinal barrier function and antigen uptake** *Microbes and Infection* **7**:997–1004 https://doi.org/10.1016/j.micinf.2005.04.003

Su L. K., Kinzler K. W., Vogelstein B., Preisinger A. C., Moser A. R., Luongo C., Gould K. A., Dove W. F (1992) **Multiple intestinal neoplasia caused by a mutation in the murine homolog of the APC gene** *Science* **256**:668–670 https://doi.org/10.1126/science.1350108

Terrin L., Agostini M., Ruvoletto M., Martini A., Pucciarelli S., Bedin C., Nitti D., Pontisso P (2017) **SerpinB3 upregulates the Cyclooxygenase-2 / beta-Catenin positive loop in colorectal cancer** *Oncotarget* **8**:15732–15743 https://doi.org/10.18632/oncotarget.14997

Tian H., Biehs B., Warming S., Leong K. G., Rangell L., Klein O. D., de Sauvage F. J. (2011) **A reserve stem cell population in small intestine renders Lgr5-positive cells dispensable** *Nature* **478**:255–259 https://doi.org/10.1038/nature10408

van der Flier L. G., Clevers H. (2009) **Stem cells, self-renewal, and differentiation in the intestinal epithelium** *Annu Rev Physiol* **71**:241–260 https://doi.org/10.1146/annurev.physiol.010908.163145

van Es J. H. *et al.* (2005) **Wnt signalling induces maturation of Paneth cells in intestinal crypts** *Nat Cell Biol* **7**:381–386 https://doi.org/10.1038/ncb1240

van Es J. H. *et al.* (2012) **Dll1+ secretory progenitor cells revert to stem cells upon crypt damage** *Nat Cell Biol* **14**:1099–1104 https://doi.org/10.1038/ncb2581

Wang A. *et al.* (2021) **An epigenetic circuit controls neurogenic programs during neocortex development** *Development* **148** https://doi.org/10.1242/dev.199772

Wang J. *et al.* (2022) **A Ctnnb1 enhancer regulates neocortical neurogenesis by controlling the abundance of intermediate progenitors** *Cell Discov* **8** https://doi.org/10.1038/s41421-022-00421-2

Wong E. S. *et al.* (2020) **Deep conservation of the enhancer regulatory code in animals** *Science* **370** https://doi.org/10.1126/science.aax8137

Xu L. *et al.* (2021) **Abnormal neocortex arealization and Sotos-like syndrome–associated behavior in Setd2 mutant mice** *Science Advances* **7** https://doi.org/10.1126/sciadv.aba1180

Yan K. S. *et al.* (2012) **The intestinal stem cell markers Bmi1 and Lgr5 identify two functionally distinct populations** *Proc Natl Acad Sci U S A* **109**:466–471 https://doi.org/10.1073/pnas.1118857109

Yao L., Liang J., Ozer A., Leung A. K.-Y., Lis J. T., Yu H (2022) **A comparison of experimental assays and analytical methods for genome-wide identification of active enhancers** *Nature Biotechnology* **40**:1056–1065 https://doi.org/10.1038/s41587-022-01211-7

Zabidi M. A., Stark A (2016) **Regulatory Enhancer-Core-Promoter Communication via Transcription Factors and Cofactors** *Trends Genet* **32**:801–814 https://doi.org/10.1016/j.tig.2016.10.003

Zhang Q., Shi X.-E., Song C., Sun S., Yang G., Li X (2015) **BAMBI Promotes C2C12 Myogenic Differentiation by Enhancing Wnt/β-Catenin Signaling** *International Journal of Molecular Sciences* **16**:17734–17745 https://doi.org/10.3390/ijms160817734

Zhang Y., Wang X (2020) **Targeting the Wnt/beta-catenin signaling pathway in cancer** *J Hematol Oncol* **13** https://doi.org/10.1186/s13045-020-00990-3

Zhao H., Ming T., Tang S., Ren S., Yang H., Liu M., Tao Q., Xu H (2022) **Wnt signaling in colorectal cancer: pathogenic role and therapeutic target** *Mol Cancer* **21** https://doi.org/10.1186/s12943-022-01616-7

Zheng G. *et al.* (2023) **Glucocorticoid receptor-mediated Nr1d1 chromatin circadian misalignment in stress-induced irritable bowel syndrome** *iScience* **26** https://doi.org/10.1016/j.isci.2023.107137

Zhu Y., Li X (2023) **Advances of Wnt Signalling Pathway in Colorectal Cancer** *Cells* **12** https://doi.org/10.3390/cells12030447

Editors

Reviewer #1 (Public review):

Summary:

Ctnnb1 encodes β-catenin, an essential component of the canonical Wnt signaling pathway. In this study, the authors identify an upstream enhancer of Ctnnb1 responsible for the specific expression level of β-catenin in the gastrointestinal track. Deletion of this promoter in mice and analyses of its association with human colorectal tumors support that it controls the dosage of Wnt signaling critical to the homeostasis in intestinal epithelia and colorectal cancers.

Strengths:

This study has provided convincing evidence to demonstrate the functions of a gastrointestinal enhancer of Ctnnb1 using combined approaches of bioinformatics, genomics, in vitro cell culture models, mouse genetics, and human genetics. The results support the idea that the dosage of Wnt/β-catenin signaling plays an important role in pathophysiological functions of intestinal epithelia. The experimental designs are solid and the data presented are of high quality. This study significantly contributes to the research fields of Wnt signaling, tissue-specific enhancers, and intestinal homeostasis.

Weaknesses:

Insufficient discussion on some findings was a major weakness in the previous submission, which has been addressed in the revised submission.

https://doi.org/10.7554/eLife.98238.2.sa3

Reviewer #2 (Public review):

Wnt signaling is the name given to a cell-communication mechanism that cells employ to inform on each other's position and identity during development. In cells that receive the Wnt signal from the extracellular environment, intracellular changes are triggered that cause the stabilization and nuclear translocation of β-catenin, a protein that can turn on groups of genes referred to as Wnt targets. Typically these are genes involved in cell proliferation. Genetic mutations that affect Wnt signaling components can therefore affect tissue expansion. Loss of function of APC is a drastic example: APC is part of the β-catenin destruction complex, and in its absence, β-catenin protein is not degraded and constitutively turns on proliferation genes, causing cancers in the colon and rectum. And here lies the importance of the finding: β-catenin has for long been considered to be regulated almost exclusively by tuning its protein turnover. In this article, a new aspect is revealed: Ctnnb1, the gene encoding for β-catenin, possesses tissue-specific regulation with transcriptional enhancers in its vicinity that drive its upregulation in intestinal stem cells. The observation that there is more active β-catenin in colorectal tumors not only because the broken APC cannot degrade it, but also because transcription of the Ctnnb1 gene occurs at higher rates, is novel and potentially game-changing. As genomic regulatory regions can be targeted, one could now envision that mutational approaches aimed at dampening Ctnnb1 transcription could be a viable additional strategy to treat Wnt-driven tumors.

https://doi.org/10.7554/eLife.98238.2.sa2

Reviewer #3 (Public review):

The authors of this paper identify an enhancer that upstream of the Ctnnb1 gene that selectively enhances expression in intestinal cells. This enhancer sequence drives expression of a reporter gene in the intestine and knockout of this enhancer attenuates Ctnnb1 expression in the intestine, while protecting mice from intestinal cancers. The human counterpart of this enhancer sequence is functional and involved in tumorigenesis. Overall, this is an excellent example of how to fully characterize a cell-specific enhancer. The strength of the study is the thorough nature of the analysis and the relevance of the data to development of intestinal tumors in both mice and humans. A minor weakness was that that loss of this enhancer does not completely compromise expression of Ctnnb1 gene in the intestine, suggesting that other elements are likely involved. The authors have now addressed this concern.

https://doi.org/10.7554/eLife.98238.2.sa1

Author response:

The following is the authors' response to the original reviews.

> ***Reviewer #1:***
>
> *(1) One issue that needs to be considered is the nomenclature of the enhancer. The authors have presented data to show this enhancer controls the expression of Ctnnb1 in the stomach, intestine, and colon tissues. However, the name proposed by the authors, ieCtnnb1 (intestinal enhancer of Ctnnb1), doesn't represent its functions. It might be more appropriate to call it a different name, such as gieCtnnb1 (gastrointestinal enhancer of Ctnnb1).*

We thank the reviewer for the insightful suggestion and agree that wholemount reporter assays indicated ieCtnnb1 and ieCTNNB1 indeed display activity in the stomach. However, in current study, we focused on the cellular distribution and the function in intestinal epithelia. After careful consideration, we reasoned that the current designation, ieCtnnb1, would be more appropriately represent its expression pattern and functions based on provided evidence. We hope the reviewer could understand our reasoning.

> *(2) The writing of this manuscript can be improved in a few places.*
>
> *a) The definitions or full names for the abbreviations of some terms, e.g., Ctnnb1, ieCtnnb1, in both abstract and main text, are needed when they first appear. Specifically, Line 108 should be moved to Lines 26 and 95. Lines 125126 are redundant. ieCtnnb1 in Line 130 needs to be defined.*

We appreciate the suggestion. In the revision, we have included the definition of Ctnnb1 and the full name of ieCtnnb1 when they first appear in the abstract and the main text. Lines 125-126 were deleted in the revision.

> *b) Line 192-194, the description of the result needs to be rewritten to reflect*

the higher expression of LacZ transcript in eGFP+ cells.

We would like to emphasize that the key point of this part is that the enhancer activity of ieCtnnb1 is present in both Lgr5-eGFP+ and Lgr5-eGFP- cells. This was validated by single-cell sequencing, which revealed the presence of LacZ transcripts in the Paneth cells. Moreover, we could not confidently conclude that eGFP+ cells have higher expression levels of LacZ, as these measurements were obtained from separate, semi-quantitative RTqPCR experiments.

> *c) More details are needed for how the data using human tumor samples were generated and how they were analyzed.*

We thank the suggestion. In the revision, we have provided additional details regarding the data and subsequent analyses of human CRC samples as follows: "We previously conducted paired analyses of chromatin immunoprecipitation sequencing (ChIP-seq) for H3K27ac and H3K4me3, alongside RNA-seq on 68 CRC samples and their adjacent normal (native) tissue (Li et al., 2021). In the current study, we performed analyses for the enrichment of H3K27ac and H3K4me3 at ieCTNNB1 and CTNNB1 promoter regions, as well as the expression levels of CTNNB1, followed by combined analyses (Figure. 5A, Figure 5 - figure supplement 1)."

> *d) The genomic structures from multiple species are presented at the bottom of Figure 1a. However, the description and explanation are lacking in both the main text and the figure legend.*

We apologize for not presenting clearly. We have added related description in the legend of Figure 1A as “The sequence conservation of the indicated species is shown at the bottom as vertical lines”. We also added an explanation in lines 162-163 of the main text: “Notably, unlike neCtnnb1, the primary sequence of ieCtnnb1 is not conserved among vertebrates (Figure 1A, bottom)”.

> ***Reviewer #2:***
>
> *(1) One of the main issues emerging during reading concerns the interpretation of the consequence of deleting the ieCtnnb1 enhancer. The authors write on line 235 that the deletion of ieCtnnb1 "undermined" Wnt signaling in the intestinal epithelium. This feels too strong, as the status of the pathway is only mildly affected, testified by the observation that mice with homozygous deletion on ieCtnnb1 are alive and well. The enhancer likely "only" drives higher Ctnnb1 expression, and it does not affect Wnt signaling by other mechanisms. The reduction of Wnt target gene expression upon its deletion is easily interpreted as the consequence of reduced β-catenin. Also the title, in my opinion, allows this ambiguity to stick in readers' minds. In other words, the authors present no evidence that the ieCtnnb1 enhancer controls Wnt signaling dosage via any mechanism other than its upregulation of Ctnnb1 expression in the intestinal epithelium. Reduced Ctnnb1, in turn, could explain the observed reduction of Wnt signaling output and the interesting downstream physiological consequences. Unless the authors think otherwise, I suggest they clarify this throughout the text, including necessary modifications to the title.*

We greatly appreciate the reviewer’s important comments and suggestion. We agree that ieCtnnb1’s direct effect on the canonical Wnt signaling is to regulate the transcription of Ctnnb1 in the intestinal epithelia. Therefore, knockout of ieCtnnb1 leads to compromised expression of Ctnnb1 and, consequently, reduced Wnt signaling. The term “undermined” is indeed too strong and has been revised to “compromised” in the revision (line 237). Similar revisions have been made throughout the manuscript. Particularly, the title was changed into “A Ctnnb1 enhancer transcriptionally regulates Wnt signaling dosage to balance homeostasis and tumorigenesis of intestinal epithelia”. However, as we state in the following point, decreased levels of β-catenin on ieCtnnb1 loss could lead to indirect effect, including the reduced expression of Bambi, which might cause a more significant decrease of nuclear β-catenin.

> *(2) It is unclear how the reduction of Ctnnb1 mRNA caused by deletion of ieCtnnb1 in mice could lead to a preferential decrease of nuclear more than membranous β-catenin (Fig. 1K and L). This might reflect a general cell autonomous reduction in Wnt signaling activation; yet, it is not clear how this could occur. Do the authors have any explanations for this?*

It's a very important question. We observed that in inCtnnb1 knockout epithelia, the expression of Bambi (BMP and activin membrane-bound inhibitor) was significantly downregulated. Since BAMBI has been reported to stabilize β-catenin and facilitate its nuclear translocation, it is likely that the reduced level of BAMBI resulting from the loss of ieCtnnb1 further decreased nuclear βcatenin. In the revision, the expression change of Bambi has been added in Figure 1M. Moreover, the related content was extensively discussed with proper citations: “We noticed that after knocking out ieCtnnb1, the level of βcatenin in the nuclei of small intestinal crypt cells of Ctnnb1Δi.enh mice decreased more significantly compared to that in the cytoplasm (49.5% vs. 29.8%). Although the loss of ieCtnnb1 should not directly lead to reduced nuclear translocation of β-catenin, RNA-seq results showed that the loss of ieCtnnb1 causes a reduction in the expression of Bambi (BMP and activin membranebound inhibitor), a target gene in the canonical Wnt signaling pathway (Figure

1M). BAMBI promotes the binding of Frizzled to Dishevelled, thereby stabilizing β-catenin and facilitating its nuclear translocation (Lin et al., 2008; Liu et al., 2014; Mai et al., 2014; Zhang et al., 2015). Thus, it is likely that the decreased level of BAMBI resulting from the loss of ieCtnnb1 further reduced nuclear βcatenin".

> *(3) In Figure 1 K-L the authors show β-catenin protein level. Why not show its mRNA?*

The mRNA levels of Ctnnb1 in small and large intestinal crypts were shown in Figure 1I and 1J, demonstrating reduced expression of Ctnnb1 upon ieCtnnb1 knockout. We hope the reviewer understands that it is unnecessary to measure the nuclear and cytosolic levels of Ctnnb1 transcripts, as the total mRNA level generally reflects the protein level.

> *(4) Concerning the GSEA of Figure 1 that includes the Wnt pathway components: a) it would be interesting to see which components and to what extent is their expression affected; b) why should the expression of Wnt components that are not Wnt target genes be affected in the first place? It is odd to see this described uncritically and used to support the idea of downregulated Wnt signaling.*

We appreciate the suggestion and apologize for any lack of clarity. The affected components of the Wnt signaling pathway and the extent of their changes are summarized in Figure 1 – figure supplement 3. Additionally, we have provided explanations for their downregulation. For instance, the reduced expression of Wnt3 and Wnt2b ligands in ieCtnnb1-KO crypts may be attributed to the decreased numbers of Paneth cells.

> *(5) In lines 251-252 the authors refer to "certain technical issues" in the isolation of cell type from the intestinal epithelium. Why this part should be obscure in the characterization of a tissue for which there are several established protocols of isolation and analysis is not clear. I would rather describe what these issues have been and how they protocol of isolation and analysis is not clear. I would rather describe what these issues have been and how they might have affected the data presented.*

We thank the reviewer for pointing this out. The single-cell preparation and sequencing of small intestinal cryptal epithelial cells were carried out largely according to reported protocols with slight modification. The enrichment of live crypt epithelial cells (EpCAM+DAPI-) by flow cytometry and cell filtering after single-cell sequencing were appropriate (Figure 2 – figure supplement 1A1C). We would like to emphasize a few points: 1) Unlike other protocols, we did not exclude immune cells, erythrocytes, or endothelial cells using negative sorting antibodies. 2) When defining cell populations, we focused exclusively on epithelial cell types and did not consider other cell types, such as immune cells. As a result, the so-called "undefined" cells include a mixture of nonepithelial cells. Indeed, markers for erythrocytes (AY036118/Erf1, PMID:12894589) and immune cells (Gm42418 and Lars2, PMID:30940803, PMID: 35659337) were the top three enriched genes in the "undefined" cluster (Figure 2 – figure supplement 1D). 3) Nonetheless, the overall findings remain robust, as key observations such as the loss of Paneth cells and reduced cell proliferation were validated through histological studies. This information has been incorporated into the revised manuscript with related references cited (lines 254-259).

> *(6) It is interesting that human SNPs exist that seem to fall within the ieCTNNB1 enhancer and affect the gastrointestinal expression of CTNNB1. Could the author report or investigate whether this SNP is present in human populations that have been considered in large-scale studies for colorectal cancer susceptibility? It seems to me a rather obvious next step of extreme importance to be ignored.*

> *(7) From Figure 5A a reader could conclude that colorectal tumor cells have a higher expression of CTNNB1 mRNA than in normal epithelium. This is the first time I have seen this observation which somewhat undermines our general understanding of Wnt-induced carcinogenesis exclusively initiated by APC mutations whereby it is β-catenin's protein level, not expression of its mRNA, of crucial importance. I find this to be potentially the most interesting observation of the current study, which could be linked to the activity of the enhancer discovered, and I suggest the authors elaborate more on this and perhaps consider it for future experimental follow-ups.*

We appreciate the comments and suggestions. We therefore added related content in the revision (lines 470-475): “Importantly, ieCTNNB1 displayed higher enhancer activity in most CRC samples collected in the study. Moreover, the SNP rs15981379 (C>T) within ieCTNNB1 is associated with the expression of CTNNB1 in the GI tract. Future population studies could investigate how the enhancer activity of ieCTNNB1 and this particular SNP are associated with CRC susceptibility and prognosis”.

> *(8) I am surprised that the authors, who seem to have dedicated lots of resources to this study, are satisfied by analyzing their ChIP experiments with qPCR rather than sequencing (Figure 6). ChIP-seq would produce a more reliable profile of the HNF4a and CREB1 binding sites on these loci and in other control regions, lending credibility to the whole experiment and binding site identification. Sequencing would also take care of the two following conceptual problems in primer design.*
>
> *First: while the strategy to divide enhancer and promoter in 6 regions to improve the resolution of their finding is commendable, I wonder how the difference in signal reflects primers' efficiency rather than HNF4/CREB1 exact positioning. The possibility of distinguishing between regions 2 and 3, for example, in a ChIP-qPCR experiment, also depends on the average DNA fragment length after sonication, a parameter that is not specified here.*
>
> *Second: what are the primers designed to detect the ieCtnnb1 enhancer amplifying in the yellow-columns samples of Figure 6G? In this sample, the enhancer is deleted, and no amplification should be possible, yet it seems that a value is obtained and set to 1 as a reference value.*

This is indeed a crucial point, and we fully agree with the reviewer that “ChIP-seq would produce a more reliable profile of the HNF4a and CREB1 binding sites on these loci and in other control regions”. However, we believe that our current ChIP-qPCR experiments have adequately addressed the potential concerns raised by the reviewers. (1) We have ensured that the DNA fragment length after sonication falls within the range of 200 bp to 500 bp, with an average length of approximately 300 bp (Author response image 1A). We have stated the point in the revised methods section (line 633). (2) We have randomly inspected 14 out of 26 primer sets used in Figure 6 and its supplemental figure (Author response image 1B-E), confirming that all primer sets demonstrate equal amplification efficiency (ranging from 90% to 110%). This information has also been included in the revised methods section (line 650). (3) Figures 6G and 6H show reduced enrichment of HNF4α (6G) and p-S133-CREB1 (6H) at the Ctnnb1 promoter in ieCtnnb1 knockout ApcMin/+ tumor tissues. The ChIP-qPCR primers used were positioned at the Ctnnb1 promoter, not at ieCtnnb1, with IgG control enrichment serving as the reference values on the Y-axes.

Author response image 1.

(A) Agarose gel electrophoresis of sonicated DNA. (B-E) Tests of amplification efficiency for primer sets used in ChIP-qPCR.

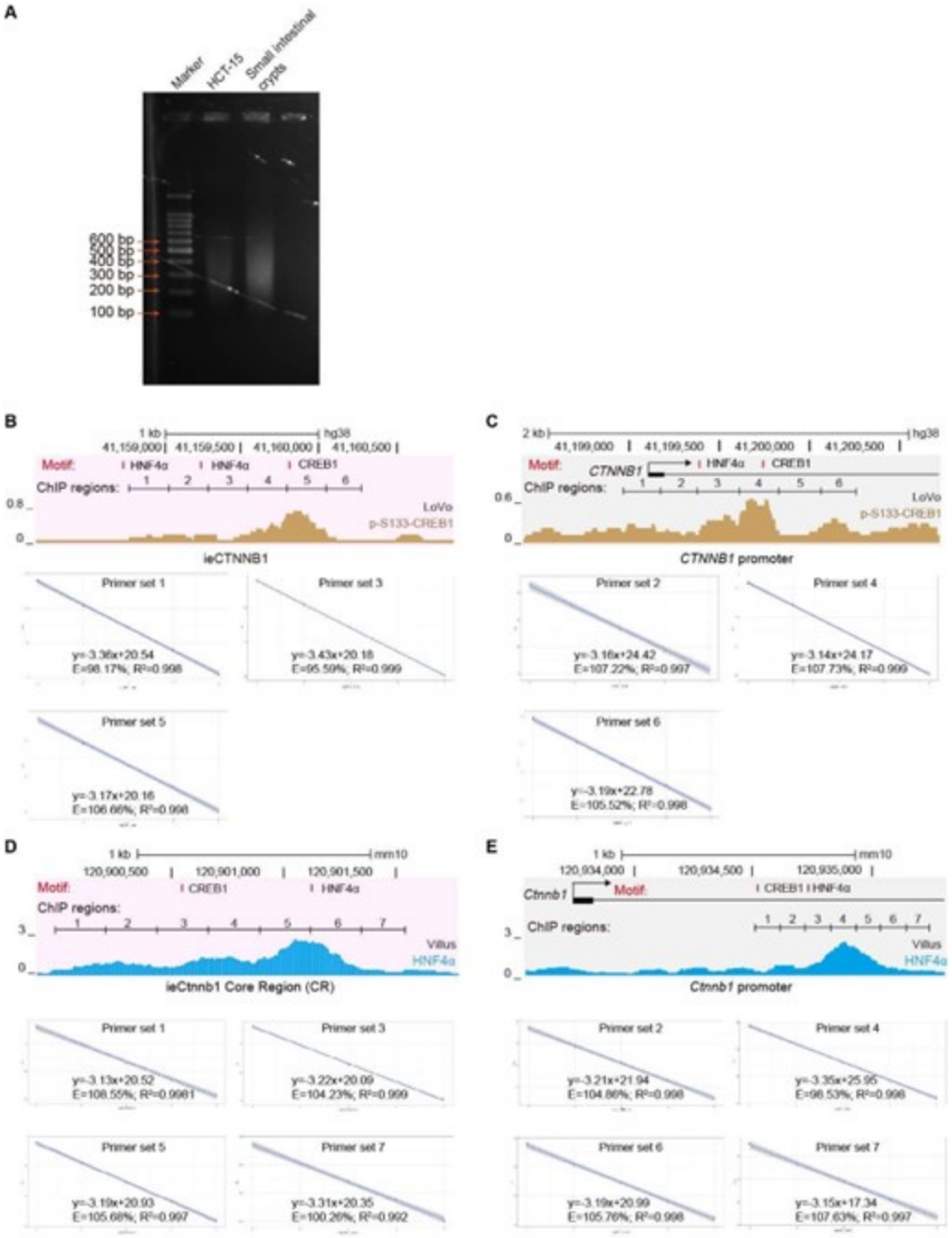

> *(9) The ChIP-qPCR showing preferential binding of pS133-CREB1 in small intestinal crypts and CHT15 cells (line 393) should be shown.*

The ChIP-qPCR results demonstrating preferential binding of p-S133-

CREB1 over CREB1 have been added in revised Figure 6C, 6D and Figure 6 – Supplement 1C.

> *(10) It is not entirely clear what the blue tracks represent at the bottom of Figures 6C-D and Figure 6 - Figure Supplement 1C-D. The ChIP-seq profiles of both CREB1 and HNF4a shown in Figures 6A and Figure 6 - Figure Supplement 1A do not seem to match. Taking HNF4a, for example from Figure 6 - Figure Supplement 1A it seems to bind on the Ctnnb1 promoter, while in Figure 6 - Figure Supplement 1D the peaks are within the first intron. I*

> *realize this might all be a problem with a different scale across figure panels, but I suggest producing a cleared figure.*

We apologize for the confusion. We have revised Figure 6C-6D, Figure 6 - figure supplement 1C-D, and the corresponding legends to enhance clarity. (1) The top panels of Figures 6C and 6D respectively highlight shaded regions of ieCTNNB1 (pink) and the CTNNB1 promoter (grey) in Figure 6A, emphasizing the enrichment of p-S133-CREB1. (2) The top panels of Figure 6 – figure supplement 1C and 1D respectively highlight shaded regions of ieCtnnb1 (pink) and the Ctnnb1 promoter (grey) in Figure 6A – figure supplement 1A, emphasizing the enrichment of HNF4α. (3) Because Figures 6C-6D and Figure 6 - figure supplement 1C-1D respectively correspond to human and mouse genomes, the positions of peaks and scales differ.

> *(11) In the intro the authors refer to "TCF-4". I suggest they use the more recent unambiguous nomenclature for this family of transcription factors and call it TCF7L2.*

TCF-4 has been changed into TCF7L2 in the revision (line 81)

> *(12) In lines 121-122, the authors write "Although numerous putative enhancers...only a fraction of them were functionally annotated". To what study/studies are the authors referring? Please provide references.*

References were added in the revision (line 124)

> *(13) In some parts the authors use strong words that should in my opinion be attenuated. Examples are: (i) at line 224, "maintains" would be better substituted with "contribute", as in the absence of ieCtnnb1, Ctnnb1 is still abundantly expressed; (ii) at line 266 "compromised" when the proliferative capacity of CFCs and TACs seems to be only mildly reduced; (iii) at line 286 "disrupts", the genes are simply downregulated.*

We thank these great suggestions. 1) On lines 224-225, the sentence was revised to: “These data suggest that ieCtnnb1 plays a specific role in regulating the transcription of Ctnnb1 in intestinal epithelia”. 2) On line 271, “compromised” were replaced with “mildly reduced”. 3) In ieCtnnb1 knockout epithelial cells of small intestine, genes related to secretory functions were decreased, while genes related to absorptive functions were increased. Therefore, the term 'disrupts' is more appropriate than 'downregulates'.

> ***Reviewer #3:***
>
> *Line 81, c-Myc should be human MYC (italics) to agree with the other human gene names in this sentence.*

c-Myc has been changed into MYC in the revision (line 82)

> *Line 215, wildtype should be wild-type.*

“wildtype” has been changed into “wild-type” in the revision (line 215)

> *Line 224, Elimination of the enhancer did not abolish expression of Ctnnb1; therefore, it would be better to say that it "helps to maintain Ctnnb1 transcription"*

The sentence was changed into “These data suggest that ieCtnnb1 plays a specific role in regulating the transcription of Ctnnb1 in intestinal epithelia” in revision (lines 224-225)

> *Line 228, perhaps "to activate transcription" is meant.*

“active” has been changed into “activate” in the revision (line 228)

> *Line 235, consider "reduced" instead of "undermined".*

“undermined” has been replaced with “compromised” in the revision (line 237)

> *Line 262, "em" dashes should be a both ends of this insertion.*
>
> *Line 298, "dysfunctional" would be better.*
>
> *Line 356, "samples were".*
>
> *Line 481, 12-hr (add hyphen).*

All above points have been optimized according to the reviewer’s suggestion.

> *Line 712, Is "poly-N" meant?*

“Poly-N” indicates undetected bases during sequencing. This explanation was added in the revision (lines 759-760).

> *Figure 1K, the GAPDH signal is not visible and that panel is unnecessary as there is an H3 control.*

Figure 1K and 1L respectively show levels of nuclear and cytoplasmic βcatenin. GAPDH and H3 were used as internal references for the cytoplasmic and nuclear fractions, respectively, confirming both robust fractionation and equal loading.

https://doi.org/10.7554/eLife.98238.2.sa0